IEEE Access
Multidisciplinary | Rapid Review | Open Access Journal

Received 15 August 2023, accepted 31 August 2023, date of publication 4 September 2023, date of current version 11 September 2023.

Digital Object Identifier 10.1109/ACCESS.2023.3311851

RESEARCH ARTICLE

Development of Efficient Energy Management Strategy to Mitigate Speed and Torque Ripples in SR Motor Through Adaptive Supervisory Self-Learning Technique for Electric Vehicles

PEMMAREDDY SAITEJA[1], BRAGADESHWARAN ASHOK[1], BYRON MASON[2], AND S. KRISHNA[1]

[1]School of Mechanical Engineering, Vellore Institute of Technology, Vellore, Tamil Nadu 632014, India
[2]Department of Aeronautical and Automotive Engineering, Loughborough University, LE11 3TU Loughborough, U.K.

Corresponding authors: Bragadeshwaran Ashok (ashokmts@gmail.com) and Byron Mason (B.Mason2@lboro.ac.uk)

This work was supported in part by the Royal Academy of Engineering under Grant RAE TSP-T2I\100100 and Grant DIA-2022-150, and in part by the Open Access funding from Engineering and Physical Sciences Research Council (EPSRC) Project under Grant EP/L014998/1.

ABSTRACT Switched reluctance motors (SRM) are receiving extensive attention from the industry because of their simple construction, high reliability and efficiency. Antithetically, controlling SRM is challenging due to its nonlinearities and variable parameters such as speed, torque, flux, etc. In this study, a novel approach is used to control the speed and torque of SRM with various controllers. This methodology integrates model-in-loop (MIL) and hardware-in-loop (HIL) simulations to evaluate the efficiency of SRM in electric vehicles (Evs). To reduce the speed variations in the SRM, PID, intelligent, hybrid, and adaptive supervisory self-learning control approaches (ASSC) are used. The mathematical models of the aforementioned controllers were created in MATLAB/Simulink, and these control approaches are used to reduce speed, torque, and current fluctuations under various load and speed conditions. In this paper, both simulation and experimental work are used to investigate the various dynamic characteristics of the SRM in Evs. From the simulation findings, the proposed ASSC controller exhibits less overshoot (1.05%), settling time (0.02s) and risetime (0.01s) than PID, intelligent and hybrid control approaches. The proposed ASSC method combines numerical data and real-time rules knowledge with ANN to predict error responses in the SR motor. Also, it is significantly reducing the speed, torque, current and flux ripples of the SRM from low to high speed with different load conditions. Further, to verify the simulation results experimental work is conducted and similar results are measured under different load and speed conditions. From experimentation, efficiency maps are developed for PID, intelligent, hybrid, and ASSCs across the entire operating range. The maps show that the controller's maximum efficiency is, respectively, 85%, 88%, 91%, and 95%. The supervisory controller is 10% more efficient than PID, intelligent, and hybrid controllers in terms of various dynamic characteristics of SRM. From the observations, both experimental and simulation results corroborated that the recommended ASSC improves the SRM efficiency.

INDEX TERMS Adaptive supervisory self-learning control technique, SRM, controller efficiency maps, model in-loop (MIL) simulation, hardware in-loop (HIL) simulation.

NOMENCLATURE

ANN	Artificial Neural Network.
GHG	Green House Gases.
BLDC Motor	Brushless Direct Current Motor.
MBC	Model-based Calibration.
DAQ	Data Acquisition System.
MFs	Membership Functions.
DoE	Design of Expert.

The associate editor coordinating the review of this manuscript and approving it for publication was Azwirman Gusrialdi.

MIL	Software In-Loop Simulation.
DTC	Direct Torque Control.
NN	Neural Network.
EMS	Energy Management Strategy.
PI	Proportional and Integral Controller.
EVs	Electric Vehicles.
PID	Proportional Integral and Derivative Controller.
FAM	Fuzzy Associative Memory.
PMSM	Permanent Magnet Synchronous Motor.
FIS	Fuzzy Inference system.
SR Motor	Switched Reluctance Motor.
FLC	Fuzzy Logic Controller.
SRM	Switched Reluctance Motor.

I. INTRODUCTION

More than ever, climate change is influencing several facets of contemporary civilization. To reverse the detrimental consequences of climate changes brought on by large Greenhouse Gas (GHG) emissions, specifically CO2, it is now widely agreed that quick action is required. Given how strongly it depends on fossil fuels, vehicle traffic is one of the main sources of such emissions. Electric vehicles (EVs) offer zero tailpipe emissions with an efficiency of up to 74-85% while ICE vehicles offer a mere efficiency of 28-30%. Due to this EVs are viewed as the answer to a more environmentally friendly transportation system that can help reduce GHG emissions [1]. Also, global EV sales increased by approximately 13% in 2022, indicating that the direction of road mobility is aligned with the goals of achieving net-zero emissions by 2050 and sustainable development goals. However, there are still certain limitations on autonomy and cost that prevent it from becoming widely accepted. The powertrain, which is the bulkiest and most expensive part of an EV, is majorly responsible for this. In EVs, the role of motors offers a great deal since these are the soul traction producing device for the entire vehicle. Due to their high-power density and sophisticated engine drive technology, permanent-magnet synchronous motors (PMSMs) are the most popular among all motor types in the automotive industry; however, the magnet materials used in these motors are typically rare earth elements like dysprosium (Dy) and neodymium (Nd). Due to this reason, the PMSMs are expensive and offer limited usage for high-end electric vehicles [2]. To overcome the limitation of magnets made of rare earth materials SRMs came into the picture which does not require any permanent magnet poles at all. Also, it can operate in harsh environments because of its simple construction, more robust design, and absence of permanent magnets. The major limitation of SRM is high torque and current fluctuation that causes vibroacoustic noise. The significant torque fluctuations are caused by strongly nonlinear electromagnetic behaviour triggered by saturation-induced nonlinear magnetic properties [3]. The control system must account for the non-linear electro-mechanical behaviour of SRM, which can be accomplished through the insightful selection of various parameter settings such as the on/off angle, shaft load, operating current, and voltage.

The researchers have been attempting to improve the SRM performance via novel control and design techniques because it is challenging to obtain precise control using only standard regulation. To eliminate torque ripples and reduce the time domain characteristics in SRM drives, several sophisticated control strategies have been put forth in the literature, including the PID, fuzzy, intelligent control, direct torque control (DTC) [4], etc. The performance of various hybrid controllers with a simple control structure has been enhanced by permitting the controller settings to respond differently to local control conditions. Also, the performance of the SRM can be enhanced by reducing torque fluctuations and accurately monitoring speed and current to their corresponding set values. For switched reluctance (SR) motors, [5] has implemented sophisticated PI and PD controllers for speed, current and torque control, respectively. The SRM speed is controlled by a PID by effectively calibrating the Particle Swarm Optimization technique and minimizing the error [6]. The PID controller is widely used in industrial process control loops, but for smooth functioning, its parameters must be tweaked. Due to their unique characteristics, nonlinear control systems like SRM that impair the performance of PID controllers give rise to more complicated instances. When the operating point shifts from the one for which the controller parameters are designed, the SRM performance degrades since the controller parameters are only useful for a small range around that point [7]. SRM control typically uses a traditional PID controller, however, when used to regulate the speed of a highly nonlinear SRM, it is challenging to get decent performance. PID controllers are appropriate for simple systems; for complicated systems, the controller must be coupled with other intelligent controllers like fuzzy or self-tuned controllers. Fuzzy Logic Controllers (FLCs) produce results that are independent of one another and are based on manually set regulations. The controller would become more sensitive by improving the membership function [8]. Many intelligent fuzzy control approaches have been presented in the literature for reducing torque vibration by altering the torque waveform, which in switch modifies the current profile [9], [10], [11], [12]. The FLC is especially helpful for controller design when the SRM is hard to mathematically represent due to its difficulty and nonlinearity. It has been demonstrated that FLC may outperform traditional PI, PD, or PID controllers while using less hardware and at a lower cost [13]. However, skilled user assistance is required during the design and implementation of these intelligent strategies. Also, these strategies are vulnerable to the experience of experts in defining problems due to a lack of system nonlinearity and mathematical complexity. Even though it can consider every practical influence when operating, too much

time and effort would be spent on training and testing the SR motor drive system.

A better option for an SR motor, which is challenging to precisely represent mathematically, is a hybrid controller which uses a simpler control logic to maintain. When the system is subjected to two distinct disturbances, such as a step change in load torque and reference speed, its performance is assessed. However, this controller encountered an uncertainty problem as a result of a sudden load disturbance [14]. Theoretical and actual performance data show that the hybrid controller can resolve the conflict between response rate and overshoot and that it performs much better than traditional PID and FLC in terms of speed, control accuracy, etc. Also, by employing a hybrid controller, the speed reaction of SRM is enhanced by 50 %, and its precision and robustness are significantly enhanced. Moreover, the static and dynamic effectiveness of the SRM system is improved [15]. The hybrid controller is therefore crucial for enhancing SRM performance and improving speed control. Although using the hybrid approach, the speed responses take a long time to reach the set value. Due to load variations, the simulation of SRM with a hybrid controller shows a larger steady-state error and settling time. It has been clearly stated that parameters such as steady-state error, overshoot, and response time are not in favor of controller efficiency during load variations [16]. The main downsides of the aforesaid strategies are complexity, slow response, high current fluctuations, and sensitivity to model accuracy. To address the aforesaid issues, this study is intending to develop an adaptive supervisory self-learning controller (ASSC) for speed, torque, and current control of switched reluctance motors. The proposed ASSC control approach is capable of quick learning and adaptation and can easily capture the process of nonlinear dynamics. By employing the ASSC control approach, the variations of speed, torque and unfavorable chattering consequences under different conditions are reduced quickly. The implementation of an ASSC technique improves the static and dynamic behaviour of the SRM in terms of various time-domain characteristics. Also, it is used to minimize torque fluctuations by modifying the current and speed profiles of the SR motor. It guarantees a low overshoot and a high accuracy transient stability with flawless steady-state performance. Moreover, it is used to address the nonlinearity and mathematical complexity issues of the SR motor. Because of its superior training and learning capabilities, it enhances the output responses of SR motor better than PID, FLC, and hybrid controllers. Finally, the supervisory self-learning controller performance characteristics are assessed and compared to PID, FLC, and Hybrid Controllers.

According to the literature review, many extant research studies on SR motor control are carried out using numerical or simulation-based methodologies. It is critical to use Hardware-in-loop (HIL) simulations to assess the real-world performance of the SR motor. Such research gives explanations and opens new possibilities in the realm of electric vehicles. Because every car manufacturer sees an EV as a future potential, a more economical and better-regulated SR motor drive has been proven to be a requirement for better EV control and performance. Due to factors such as high torque ripples, highly transient operation, running vibrations, and acoustic noise, the SR motor drive of EVs is more difficult. As a result, additional efforts are now required to further develop and optimize effective SR motor controller design. To the best of the author's knowledge, no paper has critically examined the creation of efficient controller designs for SRM through an extensive literature search. In this context, the objective of the current study is to give a broad knowledge of many alternative controllers that may be employed, such as PID, intelligent, Hybrid, etc for SRM. Since it is hard to achieve precise control of the SR motor using only traditional controllers, the researchers have focused on enlightening the performance of the SR motor by developing advanced control strategies. This study is intending to develop an adaptive supervisory self-learning controller (ASSC) using MATLAB/Simulink for reducing torque ripple by regulating the current and speed waveforms. The proposed ASSC method combines numerical data and real-time rules knowledge with ANN to predict error responses in the SR motor. Also, it is significantly reducing the speed, torque, current and flux ripples of the SRM from low to high speed with different load conditions. By adoption of the proposed control strategy in Evs, it will improve vehicle performance and achieve sustainable development goals in terms of clean energy, low energy consumption, and green transportation. Additionally, the novelty of the study is to integrate the MIL and HIL simulations to evaluate the efficiency of SR motor with different controllers in electric vehicles (Evs). In the HIL setup a 3 kW, 3-phase switched reluctance motor is used to check the efficiency of the PID, intelligent, hybrid and adaptive supervisory self-learning controllers. The controllers stated above were created in MATLAB/Simulink and are safely linked to the data acquisition card (DAC) through a USB connection. Following that, the DAQ is linked to the SR motor drive or controller via a RS-232 cable to transmit and receive real-time data under various operating conditions. Then, the output responses of the SR motor under various load and speed conditions are predicted with the above-mentioned controllers. With various output responses, the efficiency map of the SR motor with PID, intelligent, hybrid and adaptive supervisory self-learning controllers are developed. From the observations, both experimental and simulation results corroborated that the recommended ASSC improves the SRM performance. Finally, the MIL and HIL outcomes of PID, intelligent, hybrid, and proposed controllers for SRM are compared in this work.

II. PROPOSED METHODOLOGY FOR INVESTIGATION OF MIL AND HIL SIMULATIONS

The proposed methodology is used to examine the performance of the SR motor with various controllers for electric

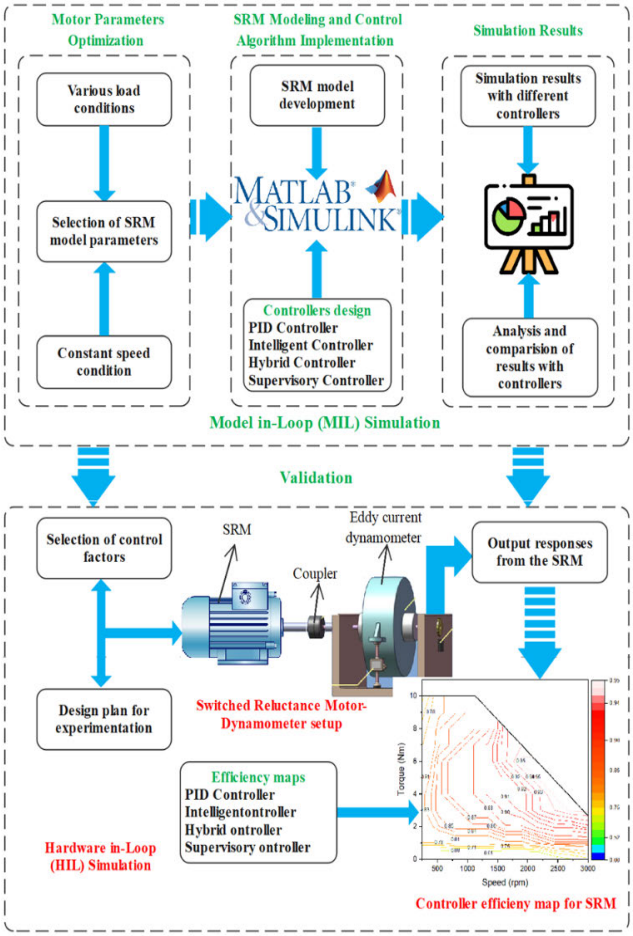

FIGURE 1. Methodology for the development of proposed controllers in MIL and HIL simulations.

vehicles. This methodology is composed of two parts: MIL simulation for speed control of SR motor using various controllers such as PID, intelligent, hybrid, and ASSC, and development of efficiency map via HIL setup. The proposed methodology and workflow of the current research are presented in Fig 1. Initially, the switched reluctance motor model parameters are optimized based on various speed and load conditions. Then, a mathematical model of the SR motor is designed using MATLAB/Simulink by integrating the controller, SR motor block, position sensor, logic circuits, and other subsystems. Due to the high nonlinearity of the SR motor, the induced torque and flux strongly influence rotor angle and currents. Thus, reducing the torque ripple requires precise turn-on and turn-off angles as well as management of the current profile. In this study, the optimal turn-on (45^0C) and off (75^0C) angles are proposed to reduce the higher torque fluctuations in the SR motor. As well, the developed SR motor model is integrated with various controllers such as PID, intelligent, hybrid and adaptive supervisory self-learning controllers. The simulation of an SR motor with aforesaid controllers yielded the following findings i) Stator current; ii) Torque; iii) Flux Linkage and iv) Speed. The output responses of the SR motor with different controllers are compared under different load conditions. From the simulation results, the ASSC approach exhibits less overshoot (1.05%), settling time (0.02s) and risetime (0.01s) than PID, intelligent and hybrid control approaches. The proposed ASSC method combines numerical data and real-time rules knowledge with ANN to predict error responses in the SR motor. Due to this, it is significantly reducing the speed, torque, current and flux ripples of the SRM from low to high speed with different load conditions.

TABLE 1. Range of the input parameters followed in experimental design.

Parameter	Motor speed	Motor load
Units	rpm	Nm
Factor type	Numeric	Numeric
Range	250-3000	0-10

Further, to verify the simulation results experimental work is conducted and similar results are measured under different load and speed conditions. This study will integrate MIL and HIL simulations to analyse the performance of SR motors with various controllers in electric vehicles (EVs). To develop an SR motor efficiency map with different controllers, this methodology integrates the different modelling tools and methods. A well-organized technique called model-based calibration (MBC) toolbox is used to ascertain how specific inputs influence future outputs. For developing an efficiency map one stage model has been preferred because here not followed any control parameter optimization. So, the operating parameters of the motor such as speed and load are regarded as independent parameters in the map development. The design plan is generated by utilizing the design of an expert (DOE) from model-based calibration of the toolbox. Based on the preliminary testing of the SR motor, acceptable tolerance limits are set for each independent input parameter like speed and load. Under the test conditions, the Sobol sequence DOE is used to capture an abundance of data on SR motor efficiency. The ranges of the input parameters for the experimental design are presented in Table 1. This design plan includes 100 trials in total, and for increased precision, the experiments are repeated under various speed and load conditions. Based on the design plan, the SR motor operated with different controllers (PID, intelligent, hybrid and supervisory controllers) under various load (0-10 Nm) and speed (0-3000 rpm) conditions. With the aforementioned controllers, the various output responses of the SR motor such as speed, current and voltage are assessed. Based on the output values, the different controller efficiency maps are developed under entire operating range of the SR motor. Finally, the stated goals will give readers knowledge as well as a critical viewpoint on the design and development of an efficient motor controller design for EVs. This study can also aid in several critical areas and propose possibilities for further investigation on the controller design of SR motors.

TABLE 2. Specifications of 6/4 3-phase switched reluctance motor for EV applications.

SNO	Parameter	Value	Units
1	Power	3	kW
2	Speed	3000	rev/min
3	Stator Resistance	0.05	Ohm
4	Viscous Friction	0.02	N m s/rad
5	Inertia	0.05	kg m^2
6	Magnetic Flux	0.486	Wb
7	Aligned Inductance	23.62	mH
8	Unaligned Inductance	0.67	mH
9	Saturated Inductance	0.15	mH
10	Maximum Current	90	A
11	Number of Stator/Rotor Pole	6/4	-
12	DC Voltage	60	V

III. MATHEMATICAL MODEL DEVELOPMENT OF SWITCHED RELUCTANCE MOTOR IN ELECTRIC VEHICLES

SRM has prominent poles on both the stator and rotor windings, with coils positioned around the stator poles and linked in diametrically opposite pairs to form the motor's phases. Reluctance torque is generated and the current direction is unipolar when a rotor pole is aligned with an excited phase. SR motor produces electromagnetic torque by exploiting the rotor angle-dependent reluctance of the permanent magnet channel attached to each phase [17]. The stator and rotor poles tend to align when a phase is energized because of the reluctance torque that is generated. When the rotor pole is equally spaced from the two neighbouring stator poles, it is said to be in the ''completely unaligned position. The rotor pole's extreme magnetic reluctance is at this position. In an aligned position, the rotor poles are completely aligned with the stator poles; this stance is referred to as the lowest reluctance of the rotor pole [18]. The winding inductance fluctuates in accordance with the current and rotor position because of double saliency. The excitation is successively changed from phase to phase as the rotor changes direction. For proper phase energization, the traditional SRM demands consistent information on real-time rotor angle. The effects of Phase coupling, the linkage flux in (Eq.2), magnetic saturation, and the fringing flux around the pole edges are ignored. The voltage (Eq.1), motion (Eq.2), and torque equation are three differential equations that may be used to define the linear systematic model of the SRM drive [16]. Also, Table 2 lists the specifications of the SRM drive selected for EV application.

The voltage equation is:

$$\text{Voltage, U} = \text{R.I} + \frac{d\lambda(t)}{dt} \tag{1}$$

where U is the applied voltage in Volts (V), R is the resistance of a coil in Ohms (Ω), 'I' is the coil unipolar-current in Amperes (A), t is the time in seconds (s) and λ is flux linkage per phase in Weber (Wb. turns).

$$\textit{Flux linkage}, \lambda = \text{I.L}(\theta, I) \tag{2}$$

where L is the coil inductance in Henry (H), θ is the different degrees of rotor angle throughout its rotation and I is the phase current of the stator. The flux-linkage (λ) is a non-linear role of stator current $I(\lambda, \theta)$ and rotor angle (θ). The stator current $I(\lambda, \theta)$ is derived from the magnetization characteristics curve, which is a nonlinear function of flux linkage (λ) and rotor position (θ).

$$\text{U} = \text{R.I} + L(\theta, I).\frac{dI(t)}{dt} + \text{emf} \tag{3}$$

The electromotive force is given by equation (4),

$$\text{emf} = \omega_n.I.\frac{\partial L(\theta, I)}{\partial \theta} \tag{4}$$

where, ω_n is the rotor angular speed in rad/s, n is the number of phases and $\omega_n = \frac{d\theta}{dt}$, where θ is the rotor position angle in degrees.

Therefore,

$$\text{Voltage, U} = \text{R.I} + L(\theta, I).\frac{dI(t)}{dt} + \omega_n.I.\frac{\partial L(\theta, I)}{\partial \theta} \tag{5}$$

The above equation (5) represents the voltage equation of the linear analytical model of the SRM drive, the three terms in the voltage equation represent the emf, inductive and resistive voltage drop, respectively. Further, the torque dynamic equation (6) of the SR motor is given by,

$$T_E\,(I, \theta) = T_L + F_V.\omega_n + J\frac{d\omega_n}{dt} \tag{6}$$

where, $T_E\,(I, \theta)$– electromagnetic torque, T_L- load torque, F_V - Viscous friction and J - moment of inertia. From the above equation, it is evident that the reduced electromagnetic torque depends on rotor position and phase current in equation (7),

$$T_E\,(I, \theta) = \frac{1}{2}I^2\frac{dL(I, \theta)}{d\theta} \tag{7}$$

The total torque equation (8) is simplified under the assumption of magnetic linearity as

$$T_{total}\,(I, \theta) = \sum\nolimits_n \frac{1}{2}I^2\frac{dL(I, \theta)}{d\theta} \tag{8}$$

Which on substituting in the mechanical equation, results in the following equation (9):

$$T_{total}\,(I, \theta) - T_L = F_V.\omega_n + J\frac{d\omega_n}{dt} \tag{9}$$

It is evident from the above equation, that the torque is equal to the product of the square of the coil current and self-inductance derivative. Since the sophisticated torque is distinct from the current sign, an optimistic torque is generated only when the derivative $\frac{\partial L(\theta, I)}{\partial \theta}$ is positive [19]. Using the aforementioned equations in the MATLAB/Simulink software, a mathematical model of a 6/4, 3-phase SRM is developed.

IV. CONTROLLER DEVELOPMENT OF SWITCHED RELUCTANCE MOTOR IN ELECTRIC VEHICLE

The controller primary goal is to control every operation in the SR motor drive and if there is a disruption in the control system, the controller restores system stability to protect the remaining equipment from further harm. This section explains how different control techniques govern SRM characteristics including speed, torque, current, etc. In this study, PID, intelligent, hybrid and ASSC approaches are examined under various conditions. The purpose of this research is to design an advanced controller using MIL simulation to control the speed, torque, flux and current of the switched reluctance motor. The proposed control systems are intended to be adaptable and to achieve the most efficient system performance.

A. PID CONTROLLER

Due to various nonlinearities of SR motor, the PID controller is giving poor dynamic performance under different operating situations. The mathematical model of the SR motor with PID controller is designed in MATLAB/Simulink. This model is built utilizing the mathematical equations derived in section III, which include the back-emf, torque, speed, etc. Initially, the input to the PID controller is the speed error, which is the difference between the reference speed and the feedback speed, and the output signal is the current command to the 3-phase inverter. This erroneous response is multiplied with gains of the PID controller such as Kp, Ki and Kd. Before modifying the gains of the controller, the non-linear SR motor control parameters must be optimized [20]. The PID gains are adjusted by using the Ziegler-Nichols approach and the continuous output control signal (u(t)) of the PID controller is presented in equation (10).

$$U(t) = K_p * e(t) + K_i * \int e(t)\,dt + K_d * \frac{d}{dt}e(t) \quad (10)$$

The performance and effectiveness of the SR motor are estimated by the turn-on and turn-off angles. The appropriate selection of turn-on and off angles will reduce the speed and torque fluctuations under different load conditions. From the simulation, the PID controller measures the different output responses including speed, torque, current, and flux. Due to its nonlinearity and mathematical complexity, the output responses of an SR motor equipped with a PID controller fluctuate more under varying operating conditions. To address these deficiencies, the intelligent controller is designed to reduce speed and torque fluctuations under different circumstances.

B. INTELLIGENT CONTROLLER

The Fuzzy Logic Controller (FLC) is widely recognized as a suitable controller for complicated linear and nonlinear systems. Numerous research publications have developed SR motor models using a variety of intelligent control strategies. In this work, an intelligent controller is developed for the speed and current control of SR motor using a fuzzy logic controller. It is used to manage a variety of input and output variables, producing effective and satisfactory results for SR motor under various conditions. At the outset, the input and output parameters of the SR motor must be specified. In this instance, the intelligent controller monitors and controls the speed errors and adjusts the outputs to match the SR motor actual and reference speed. The speed output signal is combined with the current response of the SR motor for the regulation of torque ripples based on position sensor singles [21]. Then, the intervals of input and output parameters must be described using a variety of membership functions (MFs), and it is necessary to frame the rules under a various of speed and load conditions. The input variables error (ωe) and change in error (ωce) are specified in the range of $-1 < \omega e < 1$ and $-1 < \omega ce < 1$ and the range of output variable is defined as $-1 < \omega ref < 1$. The intelligent controller employs if-then rules to transform crisp inputs into linguistic outputs and applies various control action rules (49 rules) based on the E and CE of the SR motor shown in Table 3. To implement an intelligent controller for regulating the speed of an SR motor, a tabulation strategy must be developed that maps error and change in error inputs to linguistic terms and associated control actions. The logic table aids in defining the parameters (input and output) of the intelligent controller control rules and MFs.

TABLE 3. Fuzzy associative memory used in the intelligent controller.

e/ce	NB	NM	NS	Z	PS	PM	PB
NB	NB	NB	NB	NB	NM	NS	Z
NM	NB	NB	NB	NM	NS	Z	PS
NS	NB	NB	NM	NS	Z	PS	PM
Z	NB	NM	NS	Z	PS	PM	PB
PS	NM	NS	Z	PS	PM	PB	PB
PM	NS	Z	PS	PM	PB	PB	PB
PB	Z	PS	PM	PB	PB	PB	PB

The input and output variable ranges and their MFs are determined under different conditions. It is worth noting that input and output variables have seven MFs such as Negative Big (NB), Negative Medium (NM), Negative Small (NS), Zero (Z), Positive Small (PS), Positive Medium (PM), and Positive Big (PB). The effective tuning of the different MFs may result in improved SR motor performance under varied scenarios. In the table above, the E column indicates the linguistic term for the variation between the intended and actual speed of the SR motor. Then, the CE column reveals the linguistic term linked with the error's rate of change. Finally, the output columns display the linguistic term associated to the control action that must be performed. The control actions are denoted by terms such as NB, NM, NS, Z, PB, PM, and PS. Every single cell in the outcome column represents the DOM in its respective linguistic value. This degree of memberships will be used by the intelligent control system to estimate the most suitable control action depending on the

present E and CE of the system. Additionally, to achieve the expected speed control efficiency, it necessary to ascertain the MFs and control rules experimentally via testing and simulation on the actual SR motor. It has various types of MFs based on the system type, including triangular MF, Gaussian MD, trapezoidal MF, etc. This study employs gaussian MF because it can manage nonlinear and uncertain systems such as SR motors effectively. The Gaussian MF is used to define the DOM of a given input to an ambiguous set. The Gaussian MF is constrained between 0 and 1, with its greatest value of 1 occurring at the centre (c). The degree of membership decreases as one proceeds away from the centre, based on the standard deviation value (σ). To accomplish the intended control performance, it is essential to select effective membership function parameters (centres and standard deviations) and design an ideal rule base. In order to optimize the system's response, these parameters are frequently tuned via simulation and testing. The degree of membership function control calculation is presented in equation (11).

$$y\,(p;c,\,\mu) = e^{-\frac{(p-c)^2}{2\sigma^2}} \tag{11}$$

where, p is input to estimate the DOM, c is the center for the gaussian MF and σ is the standard deviation. Initially, the parameters such as inputs, centre, and standard deviation are specified. The parameter ranges are then optimized depending on the numerous MFs (such as NB, NM, NS, Z, PS, PM, PB). Furthermore, the degree of membership is calculated in this study utilizing the exponential term described in equation (11). This work optimizes the membership function rages based on the context, and these gaussian MFs are put into a fuzzy system to improve the efficiency of the SR motor. Moreover, during the operation of an SR motor, multiple rules are simultaneously stimulated. To prevent this disruption, aggregation is used to produce a single output based on AND/OR operators. Besides that, the final phase of the intelligent controller is defuzzification, which is the transformation of the composition of fuzzy numbers into discrete values. The fuzzy output is converted to a crisp value at this stage using the centroid defuzzification approach. Finally, the goal is to implement a non-fuzzy control signal in the output system and numerous defuzzification strategies are used to provide a non-fuzzy control action in the output system to regulate output [22]. The intelligent controller is used to control the torque ripple by regulating the current and speed waveforms and also, and it enhances SR motor dynamic response more than the PID controller.

C. HYBRID CONTROLLER

Intelligent controller design and tuning are often complex since many elements must be altered, such as MFs, control rules, input, and output gains, and so on. It is also crucial to choose the correct PID controller gains, and there are numerous methods for estimating PID controller gains. Even though the controller gains may be modified, it will not improve the performance of the SR motor. As a result, a self-tuning hybrid controller is employed to update the PID gains depending on the error and change in error to manage the motor speed in both static and dynamic conditions. In this scenario, the PID controller gains are changed using an intelligent control approach. It enhances SR motor performance by choosing the appropriate rules and gain values [23]. In this study, the hybrid controller is operated in two-dimension and three-variable modes, which means it has two input and three output parameters. The inputs are E and CE, as well as the three separate outputs K_p, Ki, and Kd. The PID gains of a hybrid controller are changed using the following relations (12), (13), and (14). Also, the self-tuning hybrid controller output control signal may be described by the following equation (15).

$$K_{p2} = K_{p1} * K_p \tag{12}$$

$$K_{i2} = K_{i1} * K_i \tag{13}$$

$$K_{d2} = K_{d1} * K_d \tag{14}$$

$$UPID = K_{p2} * e\,(t) + K_{i2} * \int e\,(t)\,dt + K_{d2} * \frac{d}{dt} e(t) \tag{15}$$

where, K_{p1} is Proportional Adjustment Coefficient, K_p is Outset proportional gain, K_{i1} is Integral Adjustment Coefficient, K_i is Outset integral gain, K_{d1} is Derivative adjustment coefficient and K_d is Outset derivative gain, K_{p2}, K_{i2} and K_{d2} are the updated gains of the self-tuning hybrid controller. The adjustment coefficients K_{p1}, K_{i1}, and K_{d1} are continually adjusted dependent on the input variables. Furthermore, the initial gains of the PID controller are predicted by Ziegler-Nichol's approach based on SR motor performance under various conditions. Before that, the input and output variables are converted into linguistic variables and divided into seven levels: NB, NM, NS, Z, PS, PM, and PB. Then, the ranges of the input and output parameters are normalized between the range of [−3,3] and [−1,1]. The MFs for both the input and output variables are represented by a gaussian MF and as each of the inputs is characterized by seven linguistic values, there are $7 \times 7 = 49$ rules for each output. In total, 49×3=147 rules are required for Kp1, Ki1 and Kd1. The fine-tuned coefficients gains (Kp1, Ki1, and Kd1) of the hybrid controller are demonstrated in Table 4. The table strategy will map E, CE and PID gain output to linguistic variables and their associated control actions. In this table, 'E' stands the linguistic variables related to the variation between the desired and real speed (error), whereas 'CE' indicates the linguistic term correlated with the error's rate of change. The output cell indicates the PID controller output, which is estimated based on the current E, integral and derivative of error. The goal of the PID controller is to optimize the control operation in order to reduce steady-state failure and enhance system performance. The fuzzy output subsequently signifies the control action identified by the intelligent system depending on the E and CE inputs. The fuzzy logic system estimates the correct control action using MFs and a rule base. Then, The SR motor control action will be an amalgamation of the PID and intelligent controller outputs. The control actions are

TABLE 4. Fuzzy associative memory for hybrid controller outputs a) Kp1 b) Ki1 c) Kd1.

e/ce	NB	NM	NS	Z	PS	PM	PB
Kp1							
NB	PB	PB	PM	PM	PS	Z	Z
NM	PB	PB	PM	PS	PS	Z	NS
NS	PM	PM	PM	PS	Z	NS	NS
Z	PM	PM	PS	Z	NS	NM	NM
PS	PS	PS	Z	NS	NS	NM	NM
PM	PS	Z	NS	NM	NM	NM	NB
PB	Z	Z	NM	NM	NM	NB	NB
Ki1							
NB	NB	NB	NM	NM	NS	Z	Z
NM	NB	NB	NM	NS	NS	Z	Z
NS	NB	NM	NS	NS	Z	PS	PS
Z	NM	NM	NS	Z	PS	PM	PM
PS	NM	NS	Z	PS	PS	PM	PM
PM	Z	Z	PS	PS	PM	PM	PB
PB	Z	Z	PS	PM	PM	PB	PB
Kd1							
NB	PS	NS	NB	NB	NB	NM	PS
NM	PS	NS	NB	NM	NM	NS	Z
NS	Z	NS	NS	NM	NS	NS	Z
Z	Z	NS	NS	NS	NS	NS	Z
PS	Z	Z	Z	Z	Z	Z	Z
PM	PM	NS	PS	PS	PM	PM	PB
PB	PB	PM	PM	PM	PS	PS	PB

denoted by terms such as NB, NM, NS, Z, PB, PM, and PS. These outputs will aid in optimizing the performance of the SR motor under diverse conditions. Eventually, the linguistic variables (control actions) are processed and changed into a readable variable by the system. The optimal selection of control actions is used to control the speed and current of the SR motor by eliminating the torque ripples. Also, it enhances the dynamic response of SR motor more effectively than PID and intelligent controllers due to its superior self-tuning and generalization functionality. As a result, the hybrid controller offers a methodical approach to optimizing the PID gains and intelligent system for SR motor speed control, resulting in improved motor performance, decreased overshoot, quicker response times, and higher stability under diverse operating circumstances.

D. ADAPTIVE SUPERVISORY SELF-LEARNING CONTROLLER

The present study incorporates the use of neural networks in conjunction with a fuzzy inference system and a first-order Takagi-Sugeno fuzzy model within a supervisory self-learning controller. The integration of fuzzy logic with neural networks is a novel methodology that combines the strengths of both techniques, resulting in significant progress in the fields of nonlinear mapping, modelling, and learning. The appropriate tuning of controller settings in electric vehicles is a challenge due to the developments of SR motors. Hence, in order to enhance the efficiency of SR motors, it is imperative for controller designers to use advanced self-learning control algorithms. The supervisory self-learning controller has the capability to be used across a diverse range of control applications due to its inherent flexibility. The supervisory self-learning controller structure is organized into five interconnected neural network levels, as illustrated in Fig 2. The first layer is the input layer, with error and change in error serving as inputs to the next layer. The subsequent layer is the membership function layer, it accepts the input data from the first layer and acts as membership functions to indicate the fuzzy sets corresponding to the input variables. In this study, due to its superior performance, triangular membership function is used for the input and output layers. Further, the third level is the rule layer, which links the inputs and outputs variables with the AND operator. In this layer, each node matches the input and output variables to preconditions for fuzzy rules. Also, each node of this layer estimates the normalized input and output parameter weights. Then, the fourth layer is the output MF layer, which delivers output values based on the inference of rules. Finally, the last level is the output layer, which combines all the inputs from the preceding layer and converts the fuzzy classification results into a crisp number. It is important to establish the input membership functions and fuzzy rules before beginning the training process using a trial-and-error approach. However, the use of this approach is distinguished by a substantial allocation of time. As a result, clustering methods are used as a strategy to address this specific challenge. The current study utilizes a clustering approach to determine the initial membership functions and fuzzy rules for training input-output data sets. The number of rules in a clustering algorithm is determined by the number of membership functions given to each input variable of the controller. The system is composed of two inputs, namely error and change in error, each including seven membership functions. Consequently, a cumulative sum of 49 fuzzy rules is seen. Subsequently, via the process of watching the behaviour of the SR motor, a dataset is formed and subsequently included into the supervisory self-learning controller. The present work utilizes a hybrid learning approach in order to train and identify the datasets of a supervisory self-learning controller. The Hybrid technique integrates the back propagation and least squares error methodologies to estimate controller settings. Following the use of the hybrid learning approach to train the datasets, an error tolerance of 0.0740 is achieved after 50 iterations. Subsequently, a thorough examination of the data is conducted to identify any existing mistakes. Fig 2 illustrates the shown neural network design structure, training data set, and error value throughout the course of 50 epochs. Furthermore, the suggested supervisory controller exhibits satisfactory performance in comparison to other controllers, as shown by its configuration consisting of 98 neurons, 49 layers, and 49 rules. The hybrid control strategy is used by the supervisory controller to activate rule and neuron layers under varying situations. Every iteration is comprised of a series of forward and backward movements.

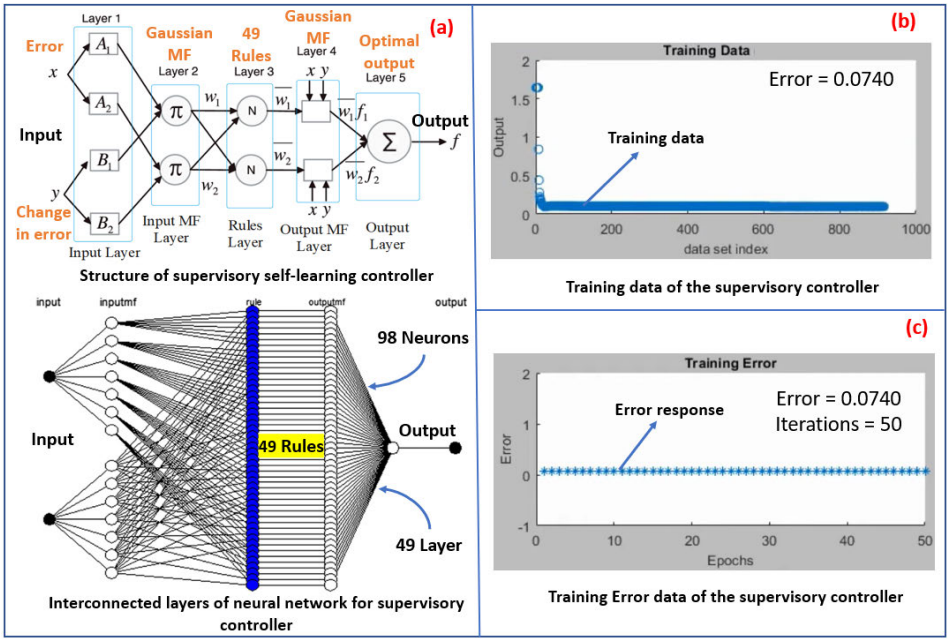

FIGURE 2. Parameters of the proposed adaptive supervisory self-learning controller (a) Structure of ASSC approach (b) Training data (c) Error response.

In the forward propagation approach, the node outputs are changed in a layer-by-layer manner starting with the presentation of the input data till reaching layer 4. The aforementioned process is iterated for each input-output training dataset, and afterwards, the final parameters are determined using the least-squares error method. Next, the backpropagation method is used to gather and revise the whole input-output dataset during the training process. Once the premise and consequence parameters of the system have been updated, the selection of the fuzzy inference system membership function and rule base takes place. Once the suitable rules have been chosen and implemented, the optimum output control signal is created. Next, the hybrid controller's answers are collected and used as the training dataset. The collected datasets are then converted into the appropriate statistics, which are dependent on the output response. After updating all the replies, the appropriate set of membership functions and rule base is selected for the fuzzy inference system. The development of a fuzzy inference system with modified membership functions has been facilitated by the use of efficient training data. Furthermore, the Simulink model for controlling an SR motor is created in MATLAB using the appropriate toolboxes as shown in Fig 3 (b). In this case, the controller is linked to a first-order Takagi-Sugeno system, and E and CE are fed into the controller. An ASSC generates the output control signals for the switching logic circuit based on the inputs. Based on the rotor position turn-on/off angles and the control signal from the supervisory controller, the circuit generates gating signals. This gating signal is used to activate the PWM inverter's IGBT switches. This mechanism governs the DC link voltage, which controls the SRM speed. Finally, the suggested ASSC strategy ensures precise torque tracking throughout the phase oscillation period [24]. The proposed speed control technique is used to minimize torque vibration by regulating the current profile and choosing appropriate turn-on/off angles. The optimal choice of turn-on and turn-off angle is identified by the inductance profile. The different region of the inductance profile and switching angle positions of the SR motor is presented in Fig 3 (a). The inductance profile depends on configuration and pole design of the SR motor. As the turn-on angle may directly impact the torque, current and speed of the SR motor under different conditions. As the SR motor accelerates, the turn on angle must increase in tandem with different current and speed levels. The SR motor output torque is non-linear as a function of inductance and current against position of the rotor. Therefore, for the SR motor to produce significant torque, each phase must be turned on during the minimal and rising inductance region ($dL/d\ominus > 0$). In addition, if the phases get fired up in the negative ($dL/d\ominus < 0$) or maximal (($dL/d\ominus = 0$) inductance region, no torque will be produced, resulting in a decrease in motor efficiency. So, the turn-on must be chosen with care to achieve a high-performance SR motor. With regard to the turn-off angle, if the phases are turned off prior to the aligned position shown in Fig 3 (a), it will be thoroughly demagnetized prior to the $dL/d\ominus < 0$. Consequently, there will be no negative torque output. In this instance, the $dL/d\ominus > 0$ will not be fully utilized, resulting in a decrease in the average output torque. Alternatively, if the phases are switched off in the fully oriented position, the current won't be completely demagnetized prior to the $dL/d\ominus < 0$, resulting in a substantial amount of current and a negative torque output. As well,

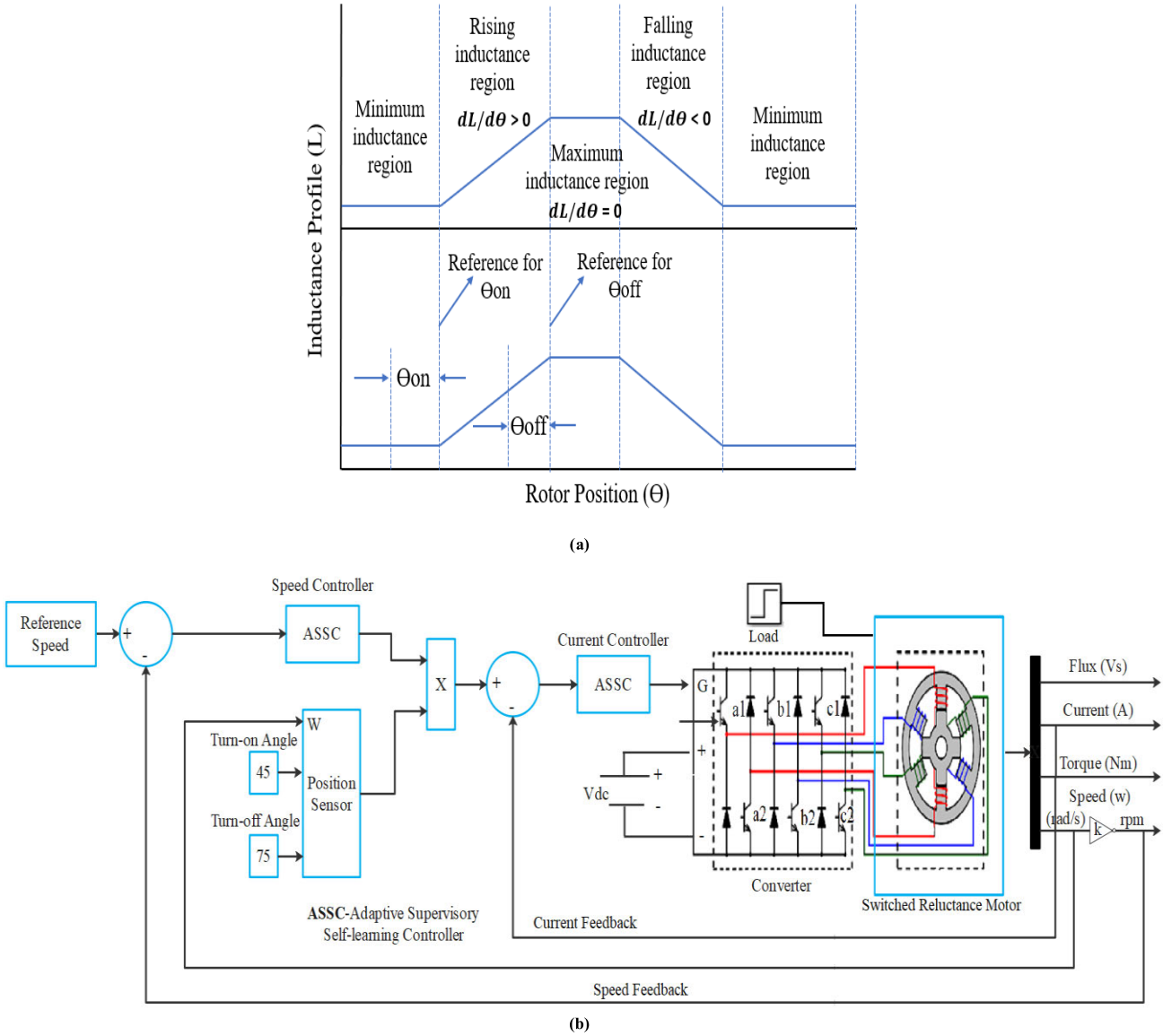

FIGURE 3. (a) Inductance profile and switching angle positions of the SR motor. (b). MATLAB/Simulink model of proposed adaptive supervisory self-learning controller for speed and current control of switched reluctance motor.

the switching turn-on and off angles are a significant impact on the torque fluctuations of the SR motor. Torque fluctuation is a crucial factor that must be taken into account, particularly when employing the SR motor for EVs. The switching positions can be adjusted off-line or on-line to improve the torque disturbance of the SR motor. An adaptive control strategy is used to identify the switching turn on (equation 16) and turn off (equation 17) angles of the SR motor under different condition [25]. By using the above equations 16 & 17, the optimal switching angles are estimated as a function of SR motor current and speed magnitudes. Using the mathematical equations (section III) and the dynamic characteristics of the SR motor, the equations 16 & 17 for the turn on and off angles are derived. Moreover, the optimal angles will help to improve the performance of the SR motor under different conditions.

$$\theta_{on} = \theta_m - \frac{-L\,(i,\theta)}{R + P_b\omega}\ln(1 - i_{ref}\frac{R + K_b\omega}{V_{DC}}) \tag{16}$$

$$\theta_{off} = 0.5\,(\theta_{on} + \theta_z) + P(1 + \omega\frac{I_{max}}{I_{Ref}}) \tag{17}$$

Despite equation 16 & 17, L-inductance, R-phase resistance, I-max-maximal current, I-ref-reference current, ω- rotor speed, V-dc-bus voltage. Based on optimal switching angles (turn-on/off), the SR motor torque, speed and current fluctuation are reduced with the proposed control system. Besides, compared to the PID, intelligent and hybrid controllers, the proposed control approach is generating maximal efficiency under different conditions.

V. MODEL IN LOOP SIMULATION RESULTS AND DISCUSSION

In MIL simulation, the mathematical model of SRM is designed in MATLAB/Simulink with various control techniques. Several experiments are conducted under various loads and constant speed conditions to determine the efficiency of SR motors equipped with PID, intelligent, hybrid, and adaptive supervisory self-learning controllers. The performance of SR motor such as speed, phase current, flux, and torque are measured and compared with different control approaches under various circumstances.

A. SPEED PERFORMANCE STUDY

Initially, the experiments are conducted with different controllers under 0% load and a rotational speed of 3000 rpm. The responses of the PID, intelligent, hybrid, and ASSC control techniques are presented in Fig 4. Existing PID, intelligent, and hybrid controllers perform poorly in terms of overshoot, settling time, and rise time when compared to the proposed ASSC. An ASSC has been demonstrated to be a superior control technique for speed control of SR motors, with the lowest overshoot, settling and risetime of 1.65%, 0.07 and 0.02s respectively.

From figure 4, the PID controller exhibits the maximum overshoot, settling and risetime of 10.55%, 0.21 and 0.09s respectively. Then, the intelligent and hybrid controllers have respective overshoot responses of 7.77% and 4.3%. From the observations, the overshoots of PID, intelligent, and hybrid controllers are significantly varying than the proposed ASSC technique. The suggested controller reaches the set speed with a less settling time and risetime than aforesaid controllers. Because it has a self-learning capability to reduce the steady-state errors in the operation of the SR motor. Moreover, to assess the effectiveness of the above-mentioned controllers, the SR motor is operating under 50 and 100 % load conditions. The speed responses of various controllers are shown in Fig 5 & 6. A step load of 50 % is applied at 0.5s of simulation time to get various time-domain properties of the SR motor. From the figure 5, the PID controller shows a maximal overshoot (8.77 %), settling time (0.12 s) and risetime (0.07 s) with a speed drop of 750 rpm under 50 % load condition.

The intelligent and hybrid controllers exhibit a minimum drop in rotational speed is 1850 and 2390 rpm compared to the PID controller. From the results, the proposed ASSC approach shows the lowest overshoot of 1.45% under medium load conditions. To verify the suggested controller performance, a 100% load is applied to an SR motor with a rotational speed of 300 rpm. From figure 6, the time-domain responses of the PID, intelligent and hybrid controllers are high fluctuating than the ASSC approach. The intelligent and hybrid controllers have a minimal overshoot such as 4.37 and 2.12 % than the PID controller. The PID controller has a maximum overshoot of 6.55% with a settling time of 0.07 s under increased load conditions. Finally, at higher loads, the proposed controller displays the lowest overshoot and settling time of 1.05 % and 0.02 s respectively. From the overall observation of speed performance with different controllers under various load conditions, the suggested ASSC approach outperforms the other controllers in terms of speed tracking, overshoot, settling time, and steady-state errors. etc. The proposed ASSC method combines numerical and real-time rules knowledge with ANN to predict data and recognize errors. Due to these factors, the ASSC results in fewer errors regarding various time-domain responses. As a result, when compared to the ASSC method, the PID, fuzzy, and hybrid controllers exhibit subpar performance with a variety of temporal domain characteristics.

B. PHASE CURRENT AND MAGNETIC FLUX PERFORMANCE STUDY

Due to significant ripples in the current and magnetic flux under different load conditions, the output responses of the PID, intelligent and hybrid controllers are unsatisfactory. Fig 7 & 10 shows the stator current and flux output response using the abovementioned controllers under a no-load condition. From figure 7, the stator current variations of the different controllers are 8.8A, 7.2A, 5.7A, and 3.8A respectively. Observations indicate that the proposed control method (ASSC) exhibits fewer current errors under no-load conditions. As well, ASSC produces a magnetic flux of 0.3Vs, while PID, intelligent, and hybrid controllers generate fluxes of 0.4Vs, 0.35Vs, and 0.32Vs respectively. Due to the nonlinearities and complex structure of the SR motor, the current and flux with PID, intelligent, and hybrid controllers are extremely unpredictable in the absence of a load when compared to the ASSC technique. Besides, a 5 Nm step load is applied to the SR motor to measure various nonlinearities in stator current and magnetic flux. The output responses of stator current and flux linkage with different controllers are shown in Fig 8 & 11. From figure 8, the stator current variations with different controllers under medium load condition are 11.5A, 10.2A, 8.5A, and 6.3A, respectively. Similarly, the magnetic flux between the stator and rotor poles of an SR motor using different controllers are 0.6Vs, 0.52Vs, 0.46Vs, and 0.42Vs. Therefore, compared to the ASSC approach, other controllers exhibit moderate to high stator current and flux fluctuations under 50 % load condition. Further, to verify the effectiveness of the foregoing controllers, a step load of 10 Nm is applied to the SR motor. The output responses of the stator current and flux are illustrated in Fig 9 & 12. The results of the stator current are 33A, 29.5A, 25.8A, and 20.7A for the PID, fuzzy, hybrid, and ASSC control approaches. Likewise, the magnetic flux variations of SR motor under full load condition are 0.8, 0.71, 0.66 and 0.61 Vs respectively. As the load on a BLDC motor increases, the results indicate that current and magnetic flux disturbances increase. Because load variations produce greater fluctuations in the BLDC motor current and flux. From the overall observation of stator current and magnet flux variations in the SR motor, the proposed ASSC approach shows a better result

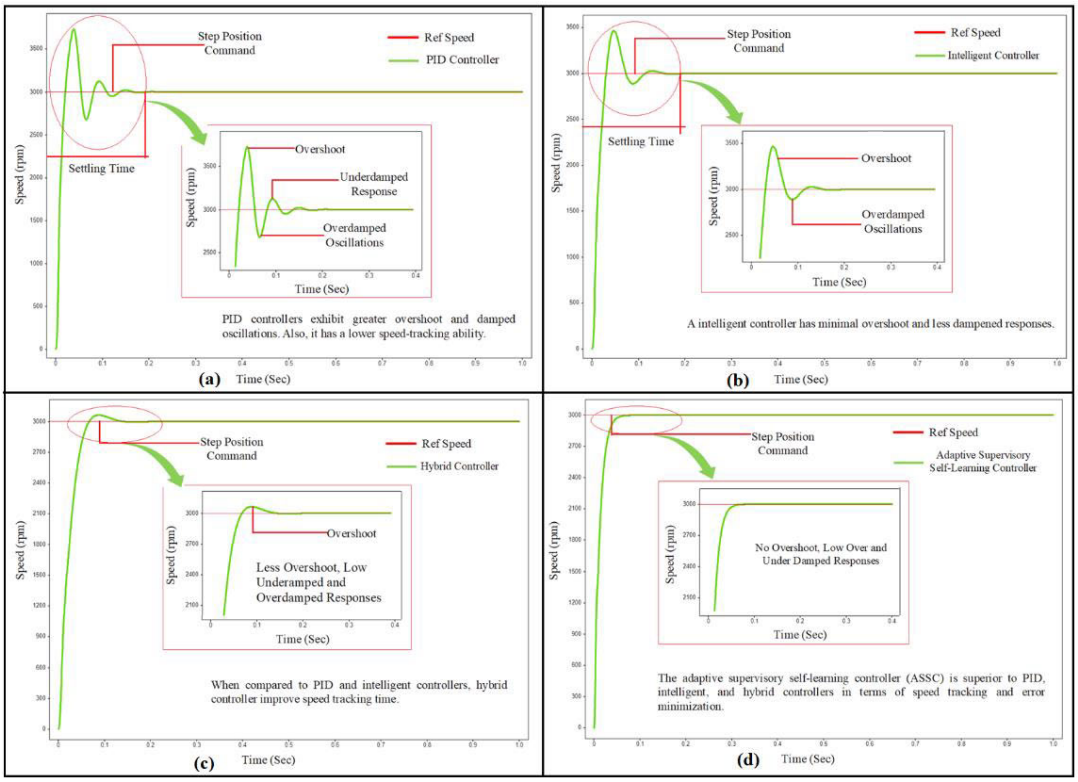

FIGURE 4. Speed response of SR Motor at No Load Condition a) PID b) Intelligent c) Hybrid d) ASSC approach.

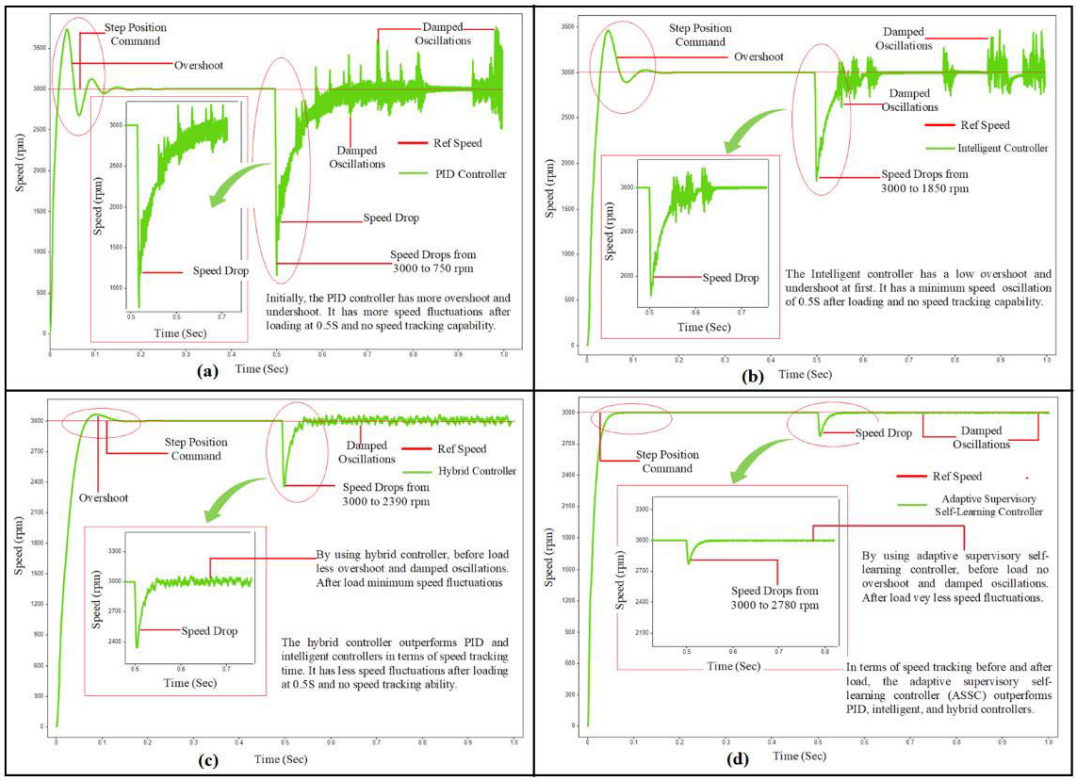

FIGURE 5. Speed response of SR Motor at 50% Load Condition a) PID b) Intelligent c) Hybrid d) ASSC approach.

than the other controllers. Due to its adjustable interpretation features for parameter tuning, the ASSC approach will reduce steady-state error fluctuations under varying load and speed conditions.

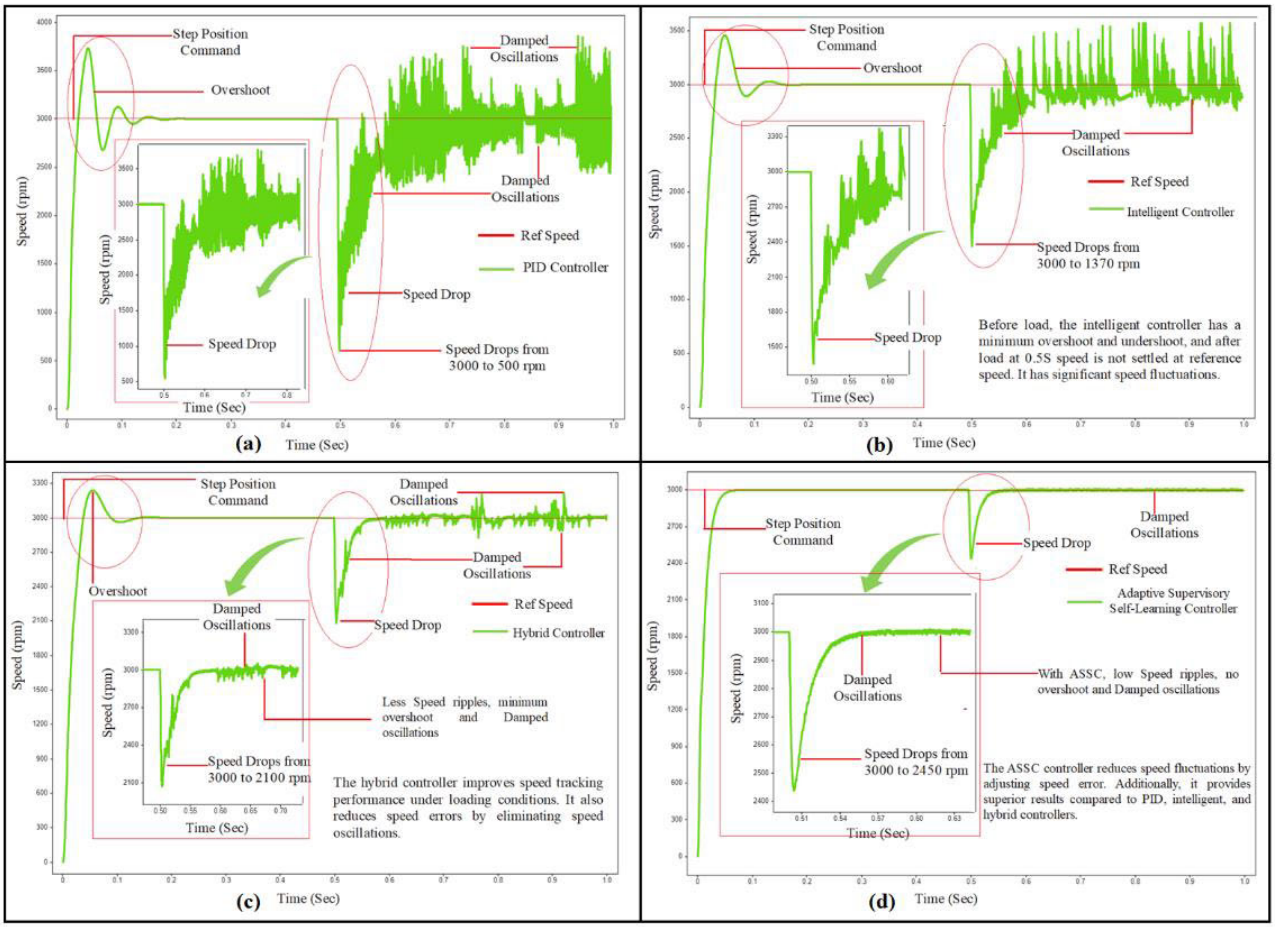

FIGURE 6. Speed response of SR Motor at 100% Load Condition a) PID b) Intelligent c) Hybrid d) ASSC approach.

C. ELECTROMAGNETIC TORQUE PERFORMANCE STUDY

Due to the variations of speed, flux, and stator phase currents, the electromagnetic torque fluctuations of an SR motor increase as the load increases. Throughout the simulation time of 0 to 1s, the SRM is driven at 3000 rpm speed under various load conditions such as 0, 5 and 10 Nm. At first, Fig 13 depicts the torque output responses of the SR motor operating at 0 Nm load under a variety of control techniques. From graph 13, the torque ripples of the PID, intelligent, hybrid and ASSC controllers are 3 Nm, 2.4 Nm, 1.9 Nm, and 1.2 Nm, respectively. It can be seen that an ASSC approach outperforms the other controllers in terms of torque vibration under no load condition. The performance and efficiency of the controllers are diminished because of the substantial torque and current variability. An ASSC is used to improve the performance of the SR motor and exhibits suitable outcomes in terms of efficiency, torque, stator current, and speed with fewer vibrations. As well, to check the performance of various controllers a step load of 5 Nm is applied to the SR motor and the output responses of the PID, intelligent, hybrid and ASSC techniques are presented in Fig 14. According to the findings, the aforesaid controllers torque fluctuations are 24.5 Nm, 15.8 Nm, 9.2 Nm, and 4.5 Nm, respectively. The suggested controllers will boost the output scaling gain by tweaking the update factor to react to the immediate load change because of the instantaneous rise in load torque. A high overshoot will be caused by the big output gain, but ultimately, the torque ripple caused by an ASSC technique is less than that caused by its traditional equivalents. Further, a load of 10 Nm is applied to SR motor to evaluate the efficiency of different control techniques.

Fig 15 represents the electromagnetic torque responses of the SR motor under the entire operating condition. According to the notes, the PID, intelligent, hybrid, and ASSC have torque responses of 34 Nm, 24 Nm, 14 Nm, and 7 Nm, respectively. The oscillations of the torque and stator currents are widely altered from low to high load situations due to the strong transient responses of the parameters. The torque ripple coefficient is lower in intelligent and hybrid controls than in PID controllers. However, it is still lower in ASSC when compared to PID, intelligent, and hybrid controllers. From the overall experimental data, The ASSC control approach produces more acceptable results than other controllers for SR motor speed, current, flux, and torque fluctuations under

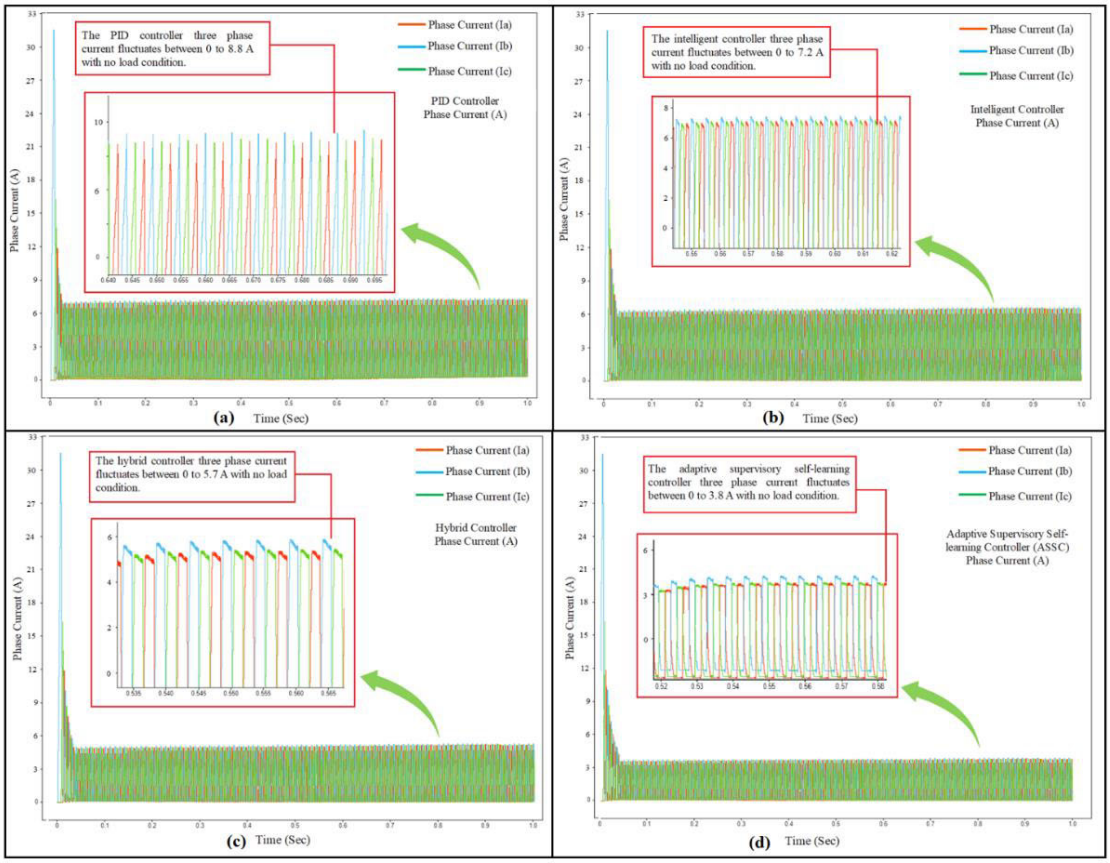

FIGURE 7. Phase current response of SR Motor at no load condition a) PID b) Intelligent c) Hybrid d) ASSC approach.

various load conditions. Due to its ability to record the non-linear structure of an operation and its adaptability, it will reduce speed and torque error variations under greater load. In essence, by employing ASSC, the performance of the SR motors will be enhanced compared to PID, intelligent, and hybrid controllers.

VI. HARDWARE IN LOOP (HIL) EXPERIMENTAL SETUP FOR SWITCHED RELUCTANCE MOTOR

For this investigation, a 3 kW, 6/4, 3-phase switched reluctance motor is used to check the efficiency of the PID, intelligent, hybrid and adaptive supervisory self-learning controllers. The SR motor is safely installed in the testbed as shown in Fig 16, and a 7.5 kW water-cooled eddy current dynamometer is securely connected to the SR motor shaft. From Fig 16, a 230 V AC voltage is supplied to the step-down transformer, which reduces the voltage to 60 V AC because the proposed SR motor operates at 60 V DC. Then, the dropped voltage is sent to the rectifier to convert 60 V AC to 60 V DC for energizing the SR motor. In this instance, a 400 V capacitor is utilized to stabilize the DC voltage of the SR motor under varying load and speed conditions. To verify the efficiency of the controllers under various conditions, the output of 60 V DC is directly connected to the drive or controller of the SR motor. As well, the controllers stated above were created in MATLAB/Simulink and are safely linked to the data acquisition card (DAC) through a USB connection. Following that, the DAQ is linked to the SR motor drive or controller via a RS 232-cable to transmit and receive real-time data under various operating conditions. Moreover, the manual load control of SR motor is possible through the eddy current dynamometer control panel. At that time, the designed control systems (PID, intelligent, etc) send 0-5 V (0-3000 rpm) speed control signals to the SR motor controller under various load (0-10 Nm) circumstances.

The output responses of the SR motor including speed, current and voltage can be predicted based on the feedback signals received from the controllers to DAQ via RS 232 cables. Based on the predicted current and voltage of SR motor under various load and speed conditions, the efficiency map of the SR motor with PID, intelligent, hybrid and adaptive supervisory self-learning controllers is developed.

VII. MODEL BASED SIMULATION AND EXPERIMENTAL VALIDATION THROUGH VARIOUS TIME-DOMAIN RESPONSES AND CONTROLLER EFFICIENCY MAPS

From the model-based simulation, the performance of the SR motor is examined using various control systems under

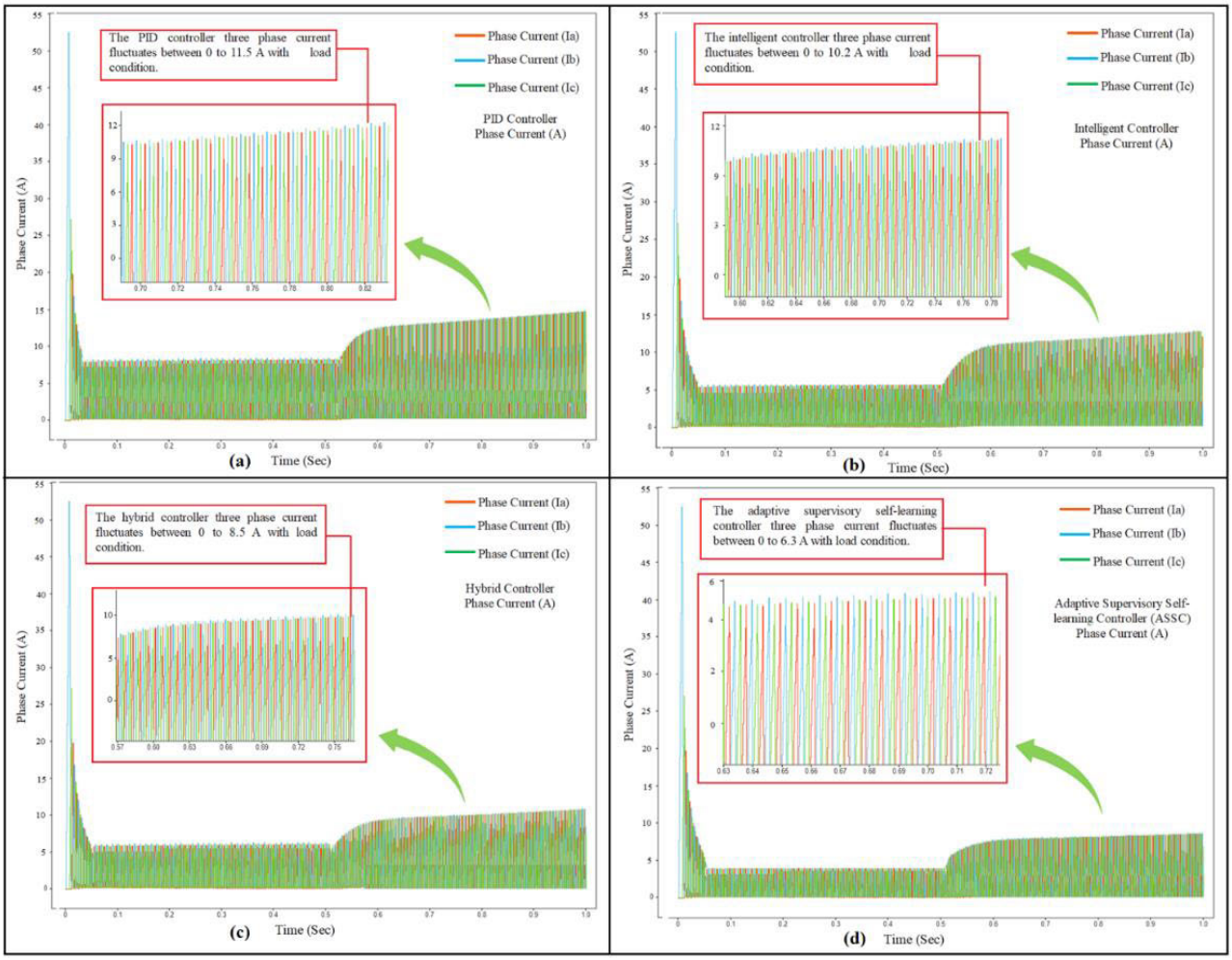

FIGURE 8. Phase current response of SR Motor at 50% Load Condition a) PID b) Intelligent c) Hybrid d) ASSC approach.

TABLE 5. Time domain characteristics of switched reluctance motor under various load conditions.

Load Condition	Controller	Overshoot (%)	Settling time (s)	Rise time (s)
No Load	PID	10.55	0.21	0.09
	Intelligent	7.77	0.16	0.07
	Hybrid	4.32	0.12	0.05
	ASSC	1.65	0.07	0.02
50% Load	PID	8.77	0.12	0.07
	Intelligent	5.35	0.08	0.05
	Hybrid	3.47	0.05	0.04
	ASSC	1.45	0.03	0.02
100% Load	PID	6.55	0.07	0.06
	Intelligent	4.37	0.05	0.05
	Hybrid	2.12	0.04	0.03
	ASSC	1.05	0.02	0.01

TABLE 6. Comparison of the effectiveness of various energy management control strategies.

Control Objectives	Controllers			
	PID	Intelligent	Hybrid	ASSC
Set speed tracking ability	✓	✓	✓	✓
Sudden load disturbances	✗	✓	✓	✓
Damping Oscillations	✗	✗	✓	✓
Overshoot response	✗	✗	✓	✓
Settling and Recovery time	✗	✗	✗	✓
Overall performance	**Low**	**Medium**	**Good**	**Best**

three distinct load circumstances. Fig 17 (a-c) compares various output responses such as overshoot, settling time, and rising time, that was acquired by running the SR motor model with PID, intelligent, hybrid and ASSC approaches. As well, Tables 5 & 6 represent the effectiveness of the above-mentioned controllers under various load conditions. From the Fig 17 (a), when the load rises, the overshoot of the aforementioned controllers decreases, and the setting and

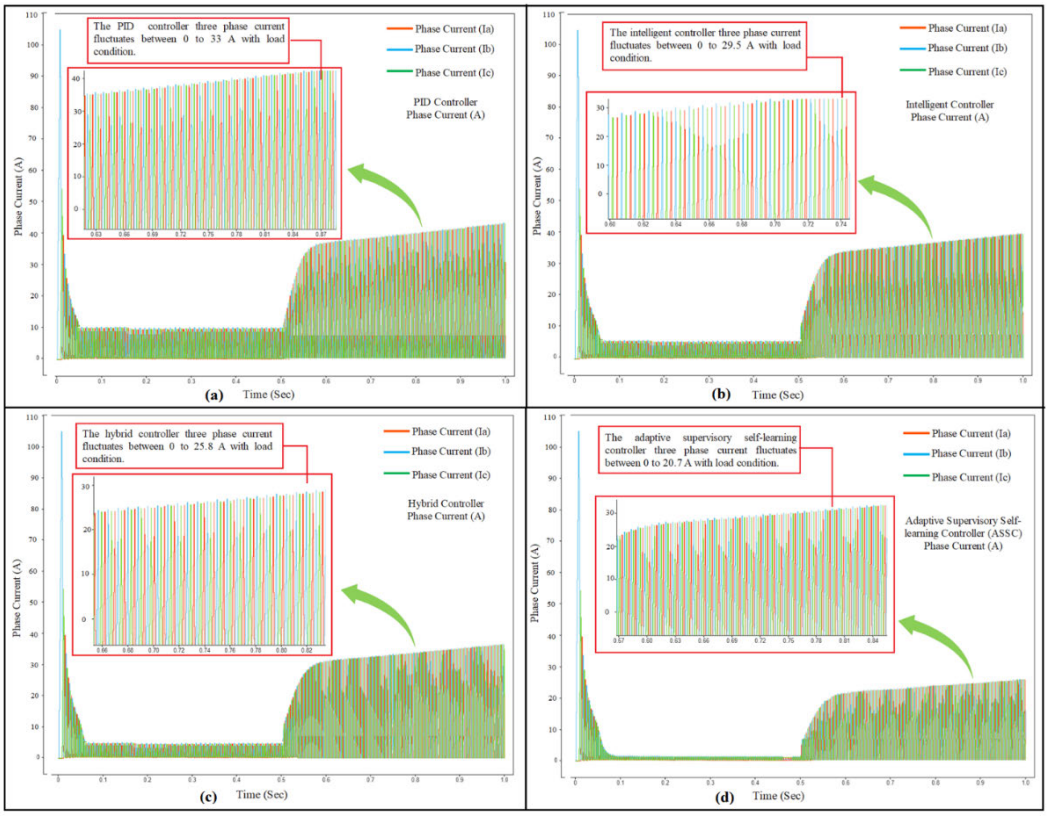

FIGURE 9. Phase current response of SR Motor at 100% Load Condition a) PID b) Intelligent c) Hybrid d) ASSC approach.

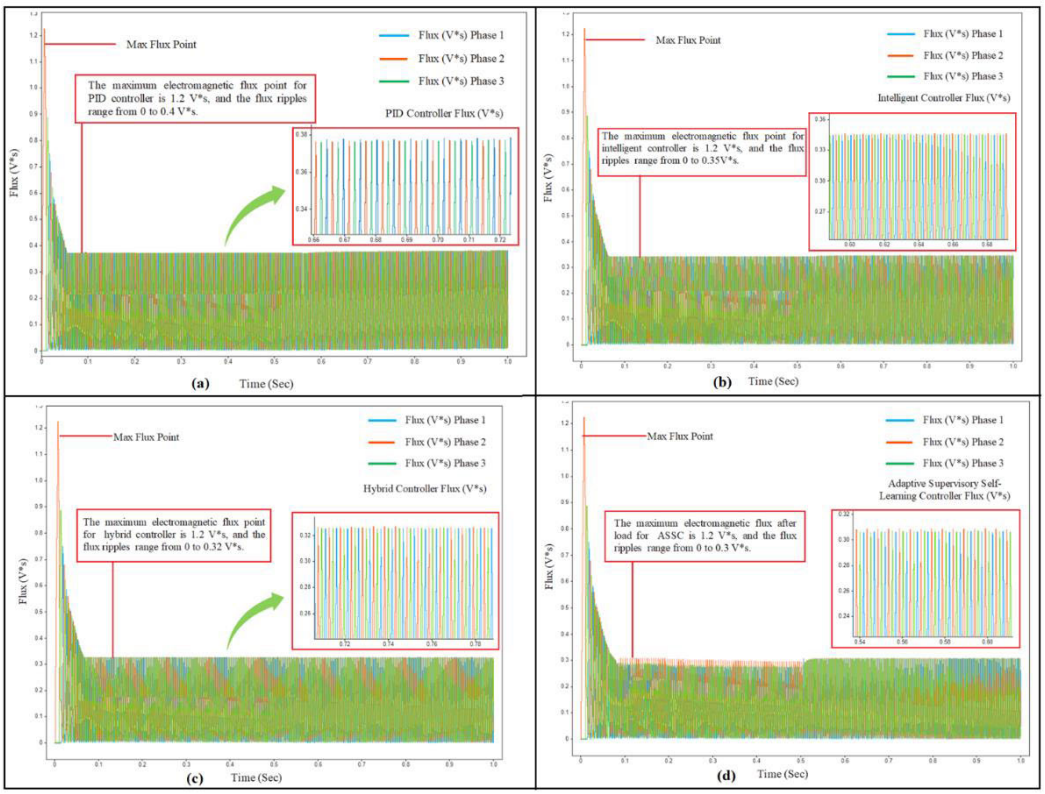

FIGURE 10. Flux response of SR Motor at No Load Condition a) PID b) Intelligent c) Hybrid d) ASSC Approach.

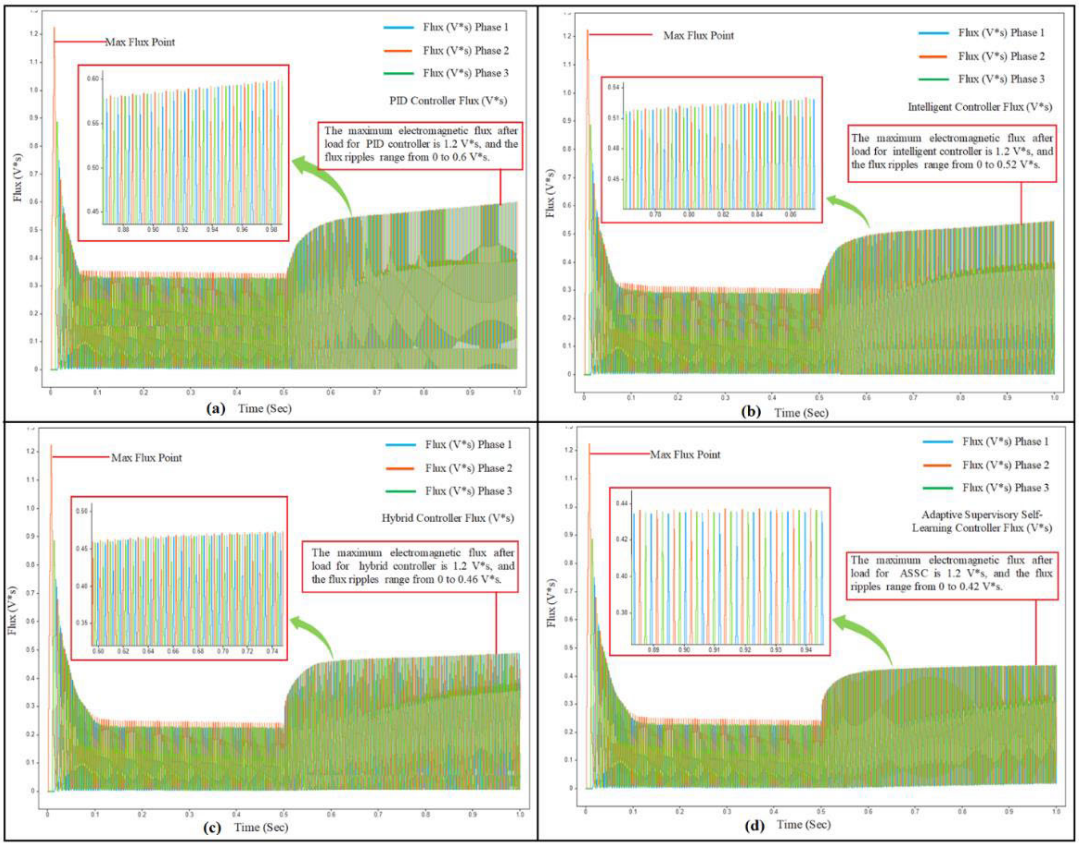

FIGURE 11. Flux response of SR Motor at 50% Load Condition a) PID b) Intelligent c) Hybrid d) ASSC approach.

recovery durations exhibit significant load-dependent variations. As the load advances from 0 to 10 Nm, the ASSC control approach overshoot seems to drop from 1.65% to 1.05%. Then, the PID, intelligent, and hybrid controller overshoot are also altering because of the load fluctuations, from 10.55% to 6.55%, 7.77% to 4.37%, and 4.32% to 2.12 respectively. Due to the high computational efficiency, speed tracking ability and interpretability, the ASSC control strategy will reduce the various error responses of SR motor under different load conditions. Subsequently, from Fig 17 (b), when increasing the load of SR motor from 0 to 10 Nm, the speed settling time and rise-time are lower for the proposed controller in all cases compared to other control strategies. The settling time of the PID, intelligent, and hybrid controllers decreases from 0.21 to 0.07s, 0.16 to 0.05s, and 0.12 to 0.04s respectively. As well, the rise-time of the aforesaid controllers are fluctuating from 0.09 to 0.06 s, 0.07 to 0.05 s, and 0.05 to 0.03 s under different load conditions. Along with, the settling and rise time of the proposed control system vary marginally between 0.07 to 0.02s and 0.02 to 0.01s. It can be asserted that the proposed controller provides superior performance in terms of various time-domain parameters of the SR motor. ASSC is utilized to achieve optimal results in terms of overshoot, settling, and rise-time based on the appropriate selection of rule base and optimal training data. Besides, the torque, current and flux ripples are varied under different load circumstances, as illustrated in Fig 17 (d-f). Also, Table 7 presents the performance parameters of the SR motor torque, phase current, and flux under various load circumstances. From the Fig 17 (d-f), the proposed control system gives optimal results than other controllers under different load conditions. It will produce

TABLE 7. Performance of electromagnetic torque, flux and phase current of SR Motr with various load condition.

Load Condition	Controller	Torque (Nm)	Phase Current (A)	Flux (V * s)
No Load	PID	3	8.8	0.4
	Intelligent	2.4	7.2	0.35
	Hybrid	1.9	5.7	0.32
	ASSC	1.2	3.8	0.3
50% Load	PID	24.5	11.5	0.6
	Intelligent	15.8	10.2	0.52
	Hybrid	9.2	8.5	0.46
	ASSC	4.5	6.3	0.42
100% Load	PID	34	33	0.8
	Intelligent	24	29.5	0.71
	Hybrid	14	25.8	0.66
	ASSC	7	20.7	0.61

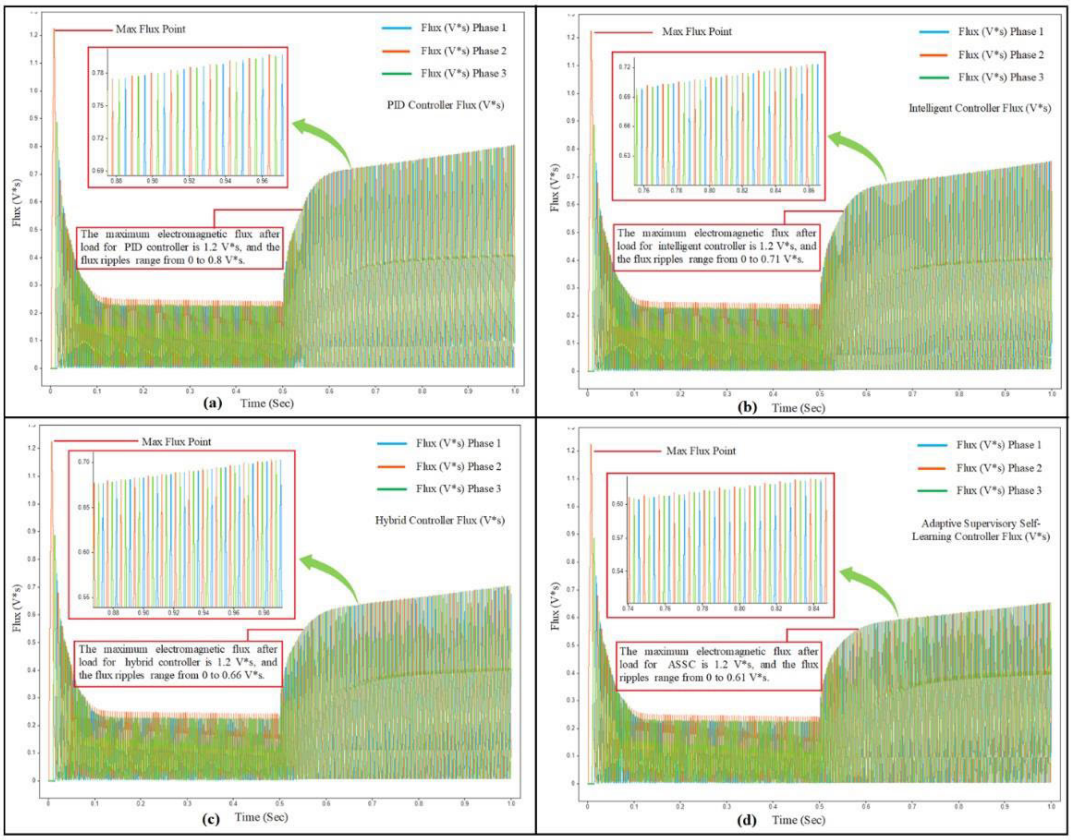

FIGURE 12. Flux response of SR Motor at 100% Load Condition a) PID b) Intelligent c) Hybrid d) ASSC approach.

less torque, current, and flux fluctuation than PID, intelligent, and hybrid controllers as a result of the optimal calibration of its parameters through the ASSC method. This research examines the experimental torque and stator current total harmonic distortion (THD) under various conditions in order to validate the effectiveness of the proposed control system. Due to switching losses, the SR motor performance will degrade under a variety of circumstances. To examine this effect, Fig 18 depicts the phase current total harmonic distortion (THD) Vs switching frequency with various controllers (PID, intelligent, hybrid and ASSC approach) under maximal load and speed condition. The estimation of the inverter switching amplitude may be obtained by using equation (18).

$$Fs = \frac{N_T}{6T} \tag{18}$$

where, N_T is the frequency of switching events of an inverter during a certain time interval (T). From the figure, as a consequence of raising the switching frequency of all controllers such as PID, intelligent, hybrid and supervisory controller, the phase current distortion is decreased. The PID controller displays the most twisted current waveform and the highest THD in comparison to other controllers. Due to the high stator flux fluctuation, the PID controller shows degraded performance of phase current and THD, which can be controlled by modifying the controller magnitudes. In addition, intelligent and hybrid controllers have a lower THD distortion waveform compared to PID controllers due to the optimal calibration of controller co-efficient under different conditions. Further, the ASSC has the lowest phase current total hormonic distortion when compared to the PID, intelligent, and hybrid controllers. Finally, the proposed controller strategy reveals superior THD performance in comparison to PID, intelligent, and hybrid controllers. Particularly the ASSC approach, which exhibits a small number of low-frequency oscillations. The main cause of the low-order vibrations in the current spectrum of ASSC approach is the sudden change in speed and load of the SR motor. By regulating the magnitudes ranges of the controller, the low-order vibration can be reduced in the SR motor. Figure 18 also demonstrates that the ASSC approach can be effectively applied to SR motors to minimize the phase current disturbance and increase the efficiency under various conditions. Moreover, Fig 19 (a-c) illustrates the experimental torque fluctuation of SR motor with various controllers under no-load, medium-load, and full-load conditions to evaluate the effectiveness of the proposed control strategy. The figure illustrates that the proposed supervisory controller exhibits lower torque ripple (1.4 Nm) across various load circumstances in comparison to the PID, intelligent, and hybrid controllers. In the absence of a load, it has been shown (Fig 19(a)) that the torque results obtained from the PID (3.4 Nm) and intelligent (2.8 Nm)

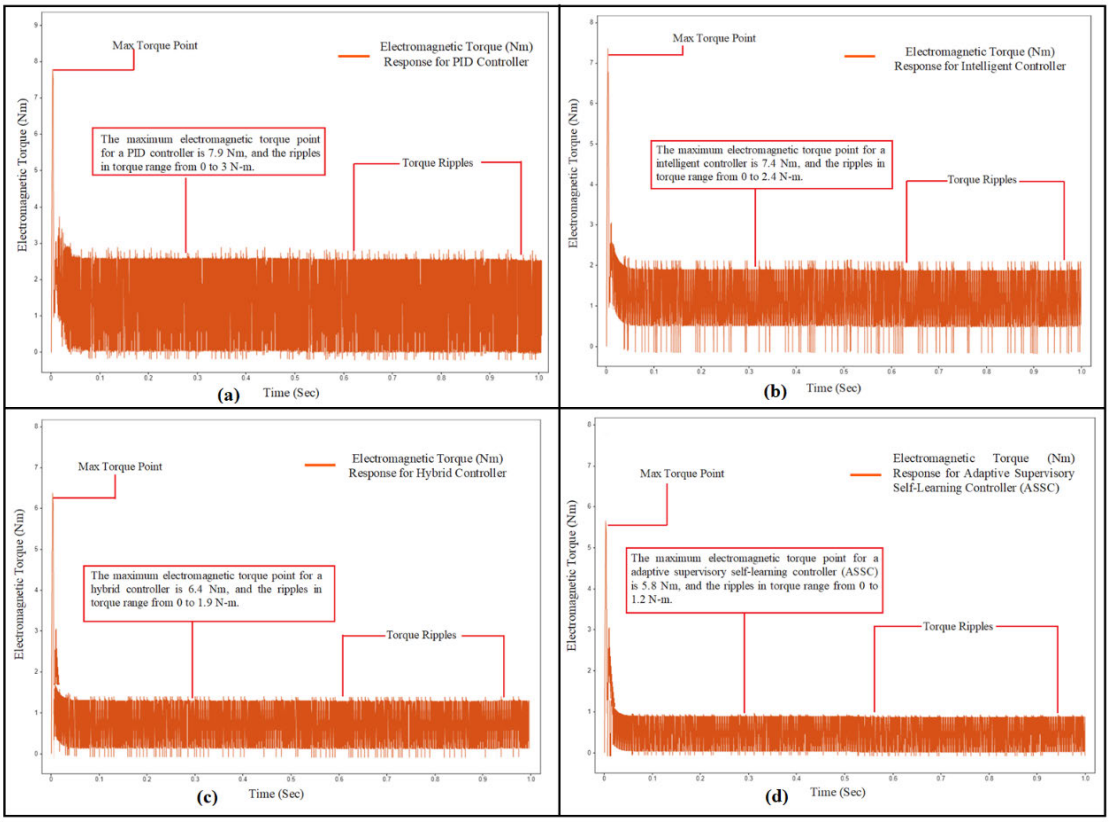

FIGURE 13. Torque response of SR Motor at No Load Condition a) PID b) Intelligent c) Hybrid d) ASSC approach.

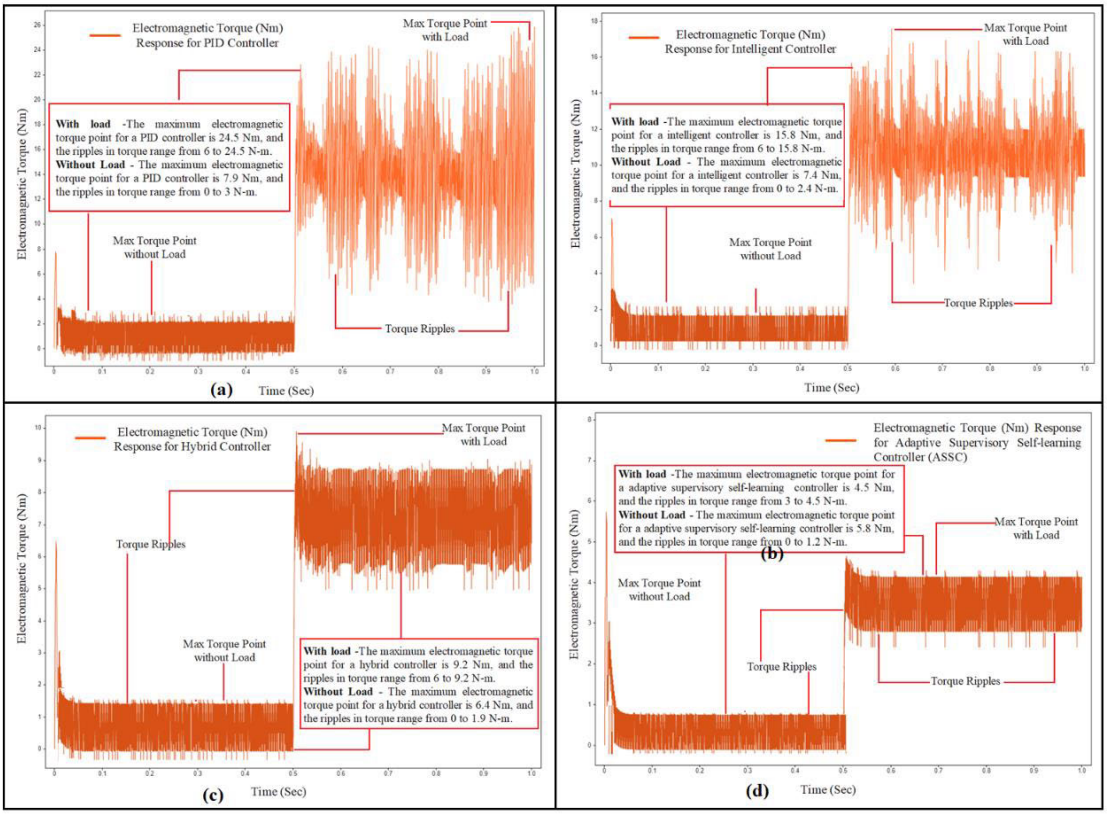

FIGURE 14. Torque response of SR Motor at 50% Load Condition a) PID b) Intelligent c) Hybrid d) ASSC approach.

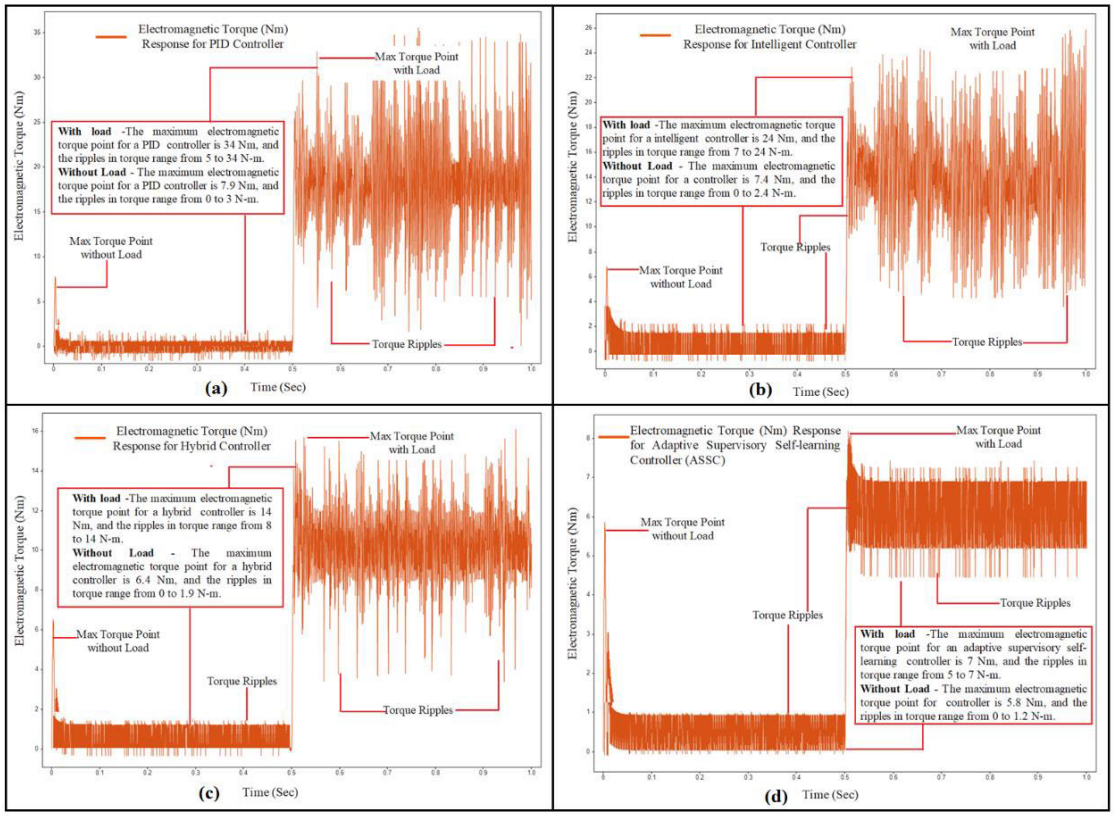

FIGURE 15. Torque response of SR Motor at 100% Load Condition a) PID b) Intelligent c) Hybrid d) ASSC approach.

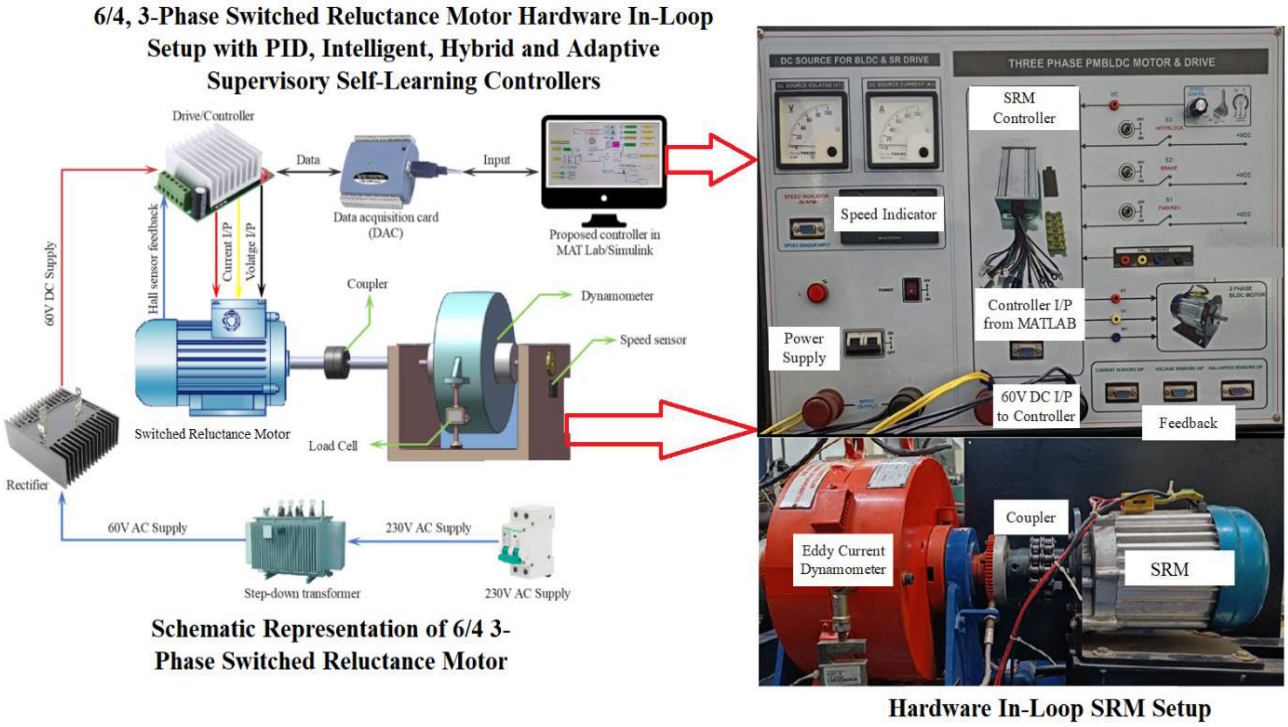

FIGURE 16. Experimental setup for 6/4 3-Phase Switched Reluctance Motor coupled with eddy current dynamometer.

controller are comparatively inferior to those achieved with the hybrid and supervisory controller. The hybrid (1.8 Nm) and supervisory (1.4 Nm) controller demonstrate a high degree of effectiveness in reducing torque ripples, while the

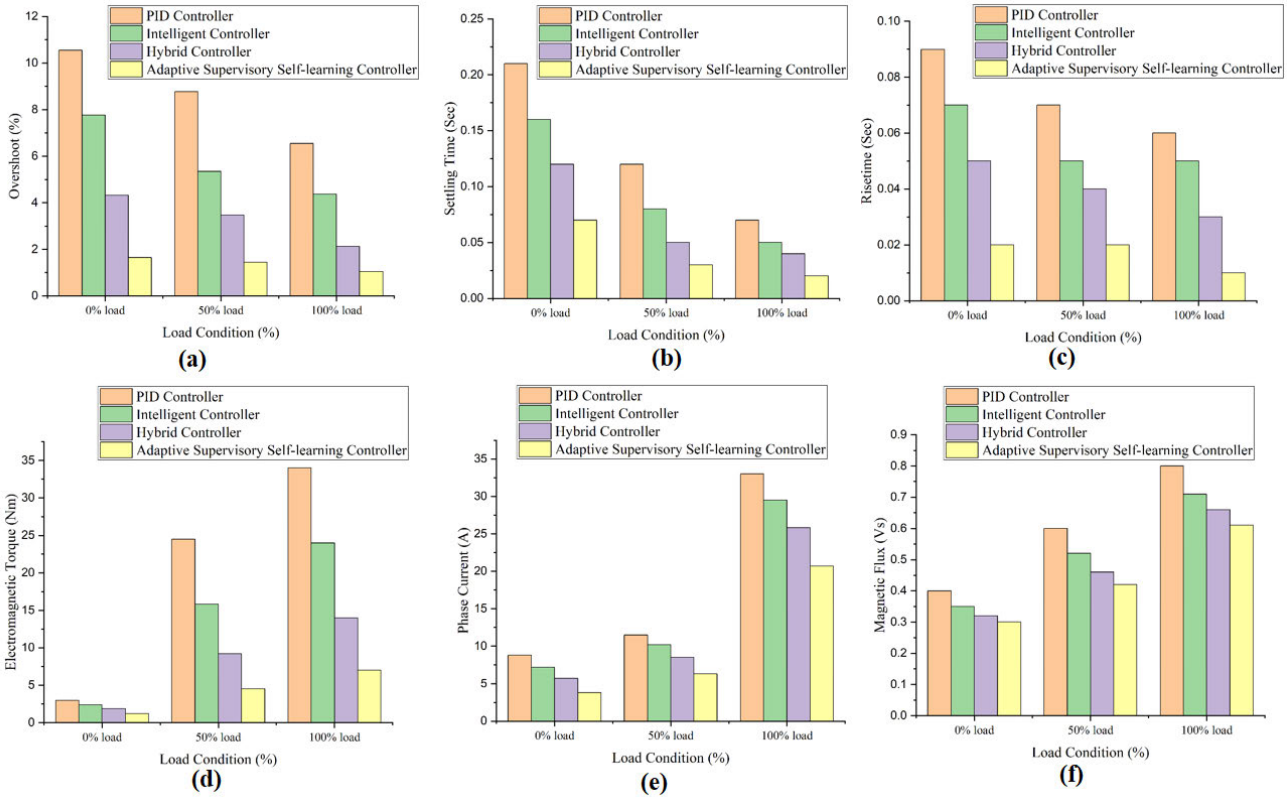

FIGURE 17. Comparison of (a) Overshoot (b) Settling Time (c) Risetime (d) Torque (e) Phase Current (f) Magnetic Flux with different controllers.

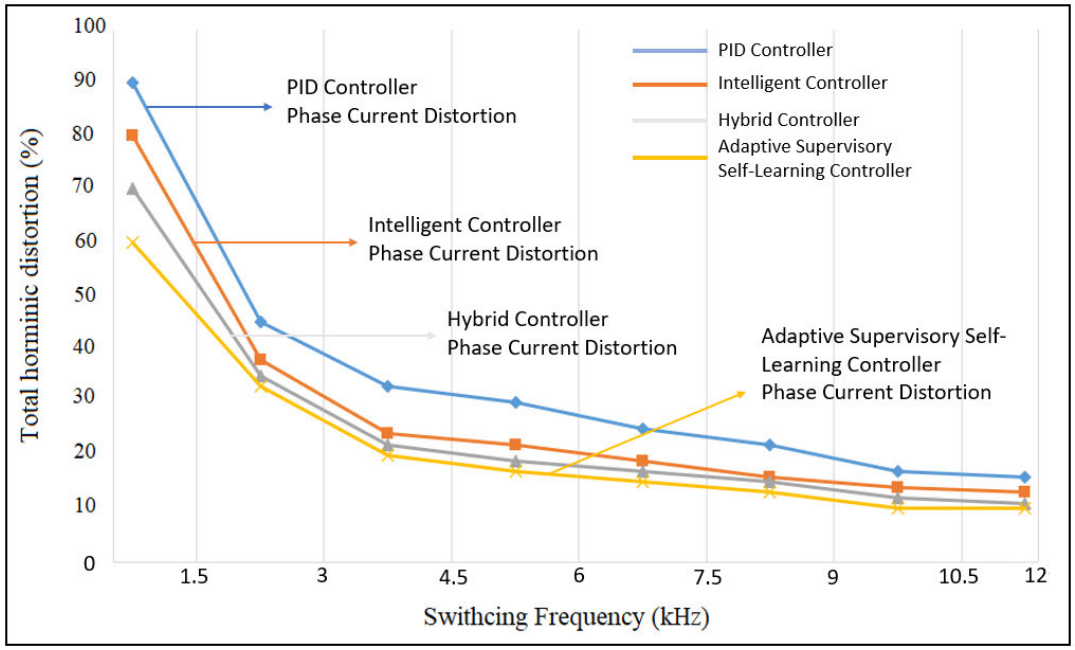

FIGURE 18. Phase current total hormonic distortion (THD) Vs switching amplitude of SR motor at higher load (10 Nm) and speed (3000 rpm) condition.

ASSC method exhibits even lower levels of torque fluctuation compared to the hybrid controller. The suggested controller exhibits slightly higher torque ripples (1.6 Nm) compared to the hybrid controller owing to fluctuations in the

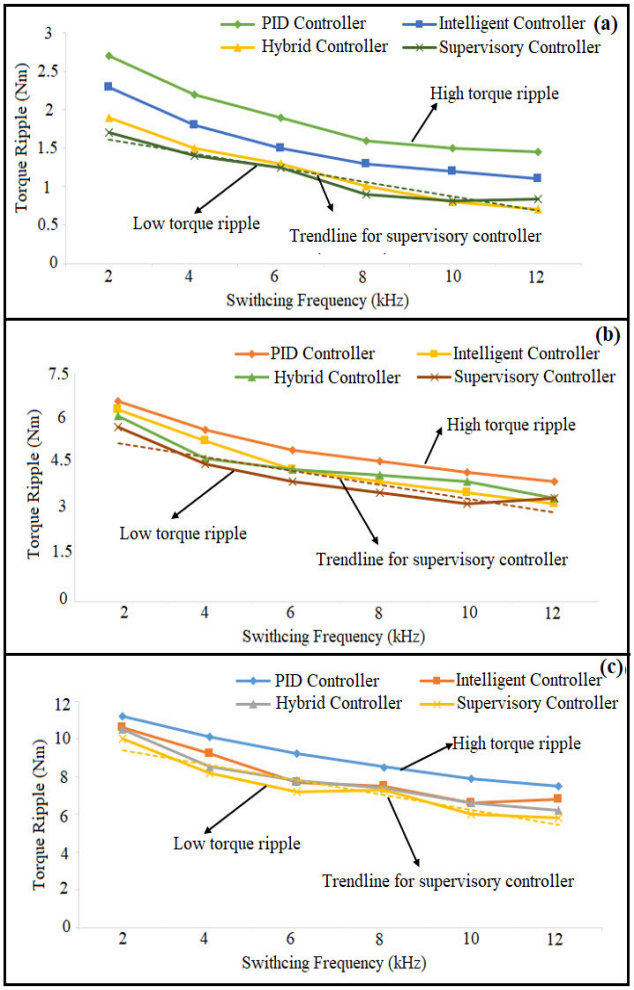

FIGURE 19. Experimental torque ripple with different controllers under same switching frequency (a) No load (b) Medium load (c) Full load.

switching frequency of the switched reluctance (SR) motor at 12 kHz. As well, under medium load condition (Fig 19(b)), the supervisory controller exhibits reduced torque variations (5.4 Nm) in comparison to other control systems. Due to the presence of nonlinearities and fluctuations in switching frequency, the SR motor under a 50% load condition produces unsatisfactory torque results. This phenomenon hinders the effectiveness of conventional PID (6.6 Nm), intelligent (6.2 Nm), and hybrid (5.8 Nm) controllers. Due to the optimal tuning of control parameter, the proposed supervisory controller demonstrates a low level of torque ripple over the whole range of switching frequencies. However, at 12kHz, the proposed controller exhibits greater torque ripple than the intelligent controller due to switching voltage fluctuations under medium load conditions. Further, the Fig 19 (c) illustrates the SR motor torque ripple under full load condition. Due to its ability to record the nonlinear structure of an operation and its adaptability, the proposed controller will reduce torque error variations under various conditions. The supervisory controller exhibits diminished torque ripples in

TABLE 8. Validation of simulation and experimental average current ripples in SR Motor.

Validation Parameters	6/4, 3 Phase Switched Reluctance Motor			
	Controllers			
	PID	Intelligent	Hybrid	ASSC
Simulation Average Current Ripples	17.7A	15.63A	13.33A	10.26A
Experimentation Average Current Ripples	17.2A	15.18A	13.23A	10.05A

comparison to other control systems. Based on an extensive examination, it can be indicated that the trendline of the supervisory controller demonstrates a decrease in torque ripple when the switching frequency is increased under various load circumstances. It is evident that the proposed controller exhibits a 60% higher level of efficiency compared to the PID controller, a 48% than intelligent controller, and a 25% than hybrid controllers Under various of load conditions. One conclusion that may be derived from the above discussion is that the proposed ASSC technique demonstrates superior performance compared to PID, intelligent, and hybrid controllers under different situations. In addition, to validate the performance of various controllers, the phase current variations are captured during simulation and experimental testing and same has been displayed in Table 8. In the simulation, the average phase current fluctuations of the SR motor with PID, intelligent, hybrid, and ASSC controllers are 17.7A, 15.63A, 13.33A, and 10.26A, respectively, under various circumstances. As well, the experimental phase current variations are measured with the foregoing controller are 17.2A, 15.18A, 13.23A, and 10.05A, respectively under the same condition. The stator current results demonstrate that the simulation and experimental phase current ripples are nearly identical for the various controllers.

More distant, to validate the results of the aforementioned controllers, experiments are conducted to develop efficiency maps under varying load and speed conditions. Fig 20 represents the PID, intelligent, hybrid and supervisory controller efficiency maps for the entire operating range of SR motor. The figure consists of two phases, namely constant torque and power regions. In initial phase, at minimum speed, the utmost torque is produced, and it remains constant up to the SR motor base speed and rated voltage (60V). In this instance, the power increases to its maximum value at the base speed and remains constant until the critical speed of the SR motor. Due to the diminished torque value after the base speed, the power of the SR motor remains constant until the critical speed. In this region, the BLDC motor reaches its highest power and efficiency with respect to the speed. The statistics show that the suggested supervisory controller is superior to other controllers in terms of efficiency. The

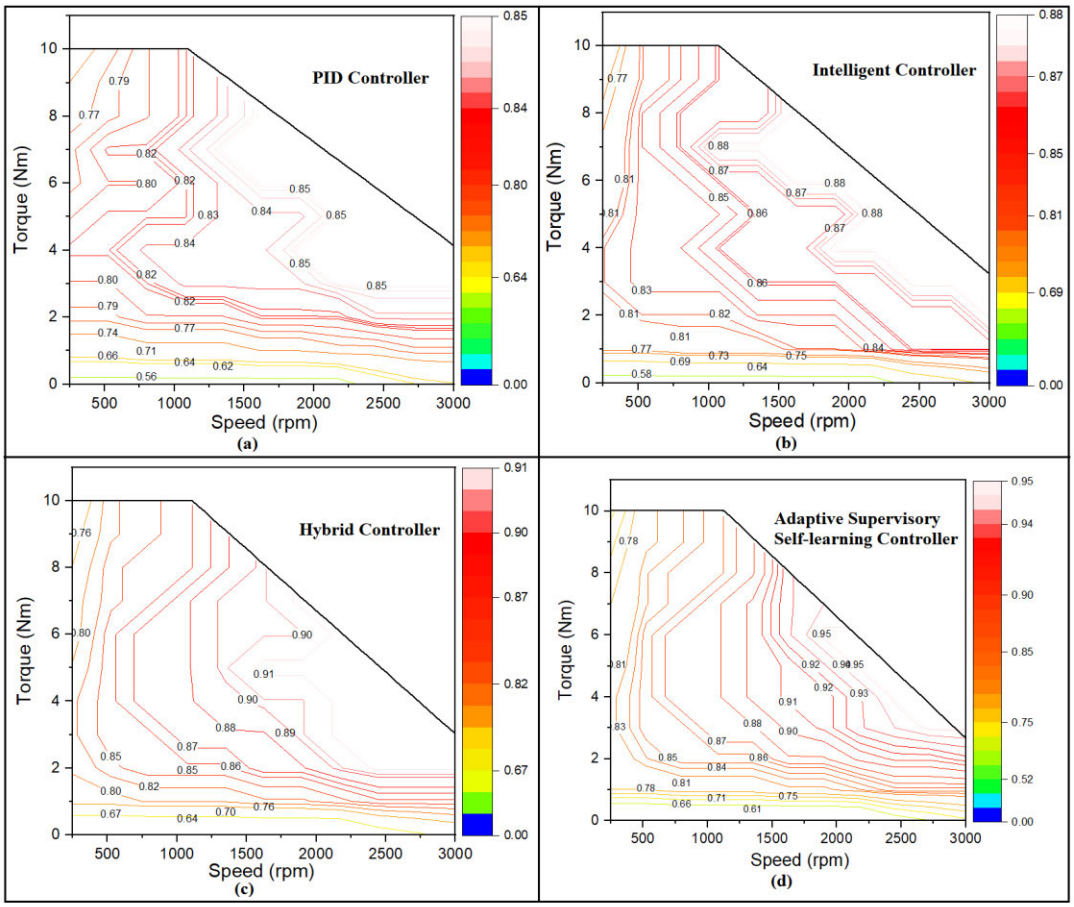

FIGURE 20. Various Controller Efficiency Maps for SRM Used in EVs (a) PID (b) Intelligent (c) Hybrid (d) ASSC approach.

maximum efficiency of PID, intelligent, hybrid, and ASSC are, in that order, 85%, 88%, 91%, and 95% respectively. From the efficiency results, the suggested adaptive supervisory self-learning controller is 10% more efficient than PID, 7% more intelligent, and 4% more than the hybrid controller. From both results, the various output responses such as speed, torque, current, and flux are varied with different controllers as the load increased. It can be observed that the suggested ASSC control approach exhibits less fluctuation than other controllers in terms of various output responses under all load circumstances. Finally, the results of the simulation and experimentation reveal that the time domain characteristics and efficiency of the SR motor are more favorable for the proposed adaptive supervisory self-learning controller.

VIII. CONCLUSION

In this study, diverse control strategies are employed to regulate the speed of an SR motor in the presence of external disturbances and parameter variations. The mathematical model of the SRM with PID, intelligent, hybrid and ASSC is designed in MATLAB/Simulink. The simulation tests are carried out with 0%, 50% and 100% load conditions at a constant speed of 3000rpm. The output responses of the SRM are overshoot, settling time, rise time, phase current, flux and electromagnetic torque are measured with different controllers. With the various time domain responses, the proposed controller displays the most efficient results than other considered controllers. As the load rises from 0 to 10 Nm, the proposed controller overshoot appears to decrease from 1.65% to 1.05%. Also, due to load variations, the overshoot of the PID, intelligent, and hybrid controllers decreases from 10.55% to 6.55%, 7.77% to 4.37%, and 4.32% to 2.12% respectively. From the above result, the suggested ASSC has less overshoot than other controllers, as well as a shorter settling time of 0.02s and a recovery time of 0.01s. According to the simulation results, the proposed control approach improves SRM performance by reducing speed, torque and current ripples. Due to its ability to record the nonlinear structure of an operation and its adaptability, it will reduce speed and torque error variations under greater load. For the validation of model-based simulation results, the phase current variations with various controllers are captured during simulation and experimentation. The results in Fig 18 (a) demonstrate that the simulation and experimental phase current ripples are nearly identical for the various controllers. Further, to evaluate the performance of the various con-

trollers, a 3 kW SR motor is safely installed in the testbed and the motor shaft is physically coupled with a 7.5 kW rated water-cooled eddy current dynamometer. The SRM test bed is operated with different designed controllers in the MATLAB/Simulink under varying load and speed conditions. From the responses, the energy-saving motor efficiency map is developed for the whole operating range of SRM with different controllers. The maximum efficiencies of the various controllers are 85%, 88%, 91%, and 95% respectively. From the experimental results, the suggested adaptive supervisory self-learning controller is 10% more efficient than PID, 7% more intelligent, and 4% more than the hybrid controller. From both results, the various output responses such as speed, torque, current, and flux are varied with different controllers as the load increased. It can be observed that the suggested ASSC control approach exhibits less fluctuation than other controllers in terms of various output responses under all load circumstances. The both experimental and simulation results validated that the recommended ASSC approach improves the SR motor efficiency. However, the proposed controller efficiency is highly dependent on training data, and this data always influences the performance of the suggested controller. This may be a shortcoming of the proposed controller, and some specific optimization techniques, as well as sophisticated controllers such as multi adaptive neuro-fuzzy inference system (MANFIS), might be employed for training the data to obtain efficient and stable performance of the proposed controller, which is worthy of further investigation.

REFERENCES

[1] H. A. Maksoud, "Torque ripple minimization of a switched reluctance motor using a torque sharing function based on the overlap control technique," *Eng., Technol. Appl. Sci. Res.*, vol. 10, no. 2, pp. 5371–5376, Apr. 2020, doi: 10.48084/etasr.3389.

[2] R. Abdelfadil and L. Számel, "Predictive direct torque control of switched reluctance motor for electric vehicles drives," *Periodica Polytechnica Electr. Eng. Comput. Sci.*, pp. 264–273, Jul. 2020, doi: 10.3311/PPee.15496.

[3] X. Tian, Y. Cai, X. Sun, Z. Zhu, and Y. Xu, "A novel energy management strategy for plug-in hybrid electric buses based on model predictive control and estimation of distribution algorithm," *IEEE/ASME Trans. Mechatronics*, vol. 27, no. 6, pp. 4350–4361, Dec. 2022, doi: 10.1109/TMECH.2022.3156150.

[4] M. Hamouda, A. A. Menaem, H. Rezk, M. N. Ibrahim, and L. Számel, "Numerical estimation of switched reluctance motor excitation parameters based on a simplified structure average torque control strategy for electric vehicles," *Mathematics*, vol. 8, no. 8, p. 1213, Jul. 2020, doi: 10.3390/math8081213.

[5] F. Al-Amyal, L. Számel, and M. Hamouda, "An enhanced direct instantaneous torque control of switched reluctance motor drives using ant colony optimization," *Ain Shams Eng. J.*, vol. 14, no. 5, May 2023, Art. no. 101967, doi: 10.1016/j.asej.2022.101967.

[6] V. Abhijith, M. J. Hossain, G. Lei, P. A. Sreelekha, T. P. Monichan, and S. V. Rao, "Hybrid switched reluctance motors for electric vehicle applications with high torque capability without permanent magnet," *Energies*, vol. 15, no. 21, p. 7931, Oct. 2022, doi: 10.3390/en15217931.

[7] N. Saha and S. Panda, "Speed control with torque ripple reduction of switched reluctance motor by hybrid many optimizing liaison gravitational search technique," *Eng. Sci. Technol., Int. J.*, vol. 20, no. 3, pp. 909–921, Jun. 2017, doi: 10.1016/j.jestch.2016.11.018.

[8] K. K. Nimisha and R. Senthilkumar, "Optimal tuning of PID controller for switched reluctance motor speed control using particle swarm optimization," in *Proc. Int. Conf. Control, Power, Commun. Comput. Technol. (ICCPCCT)*, 2018, pp. 487–491, doi: 10.1109/ICCPCCT.2018.8574234.

[9] N. Saha, A. K. Panda, and S. Panda, "Speed control with torque ripple reduction of switched reluctance motor by many optimizing liaison technique," *J. Electr. Syst. Inf. Technol.*, vol. 5, no. 3, pp. 829–842, Dec. 2018, doi: 10.1016/j.jesit.2016.12.013.

[10] R. M. Pindoriya, B. S. Rajpurohit, R. Kumar, and K. N. Srivastava, "Comparative analysis of permanent magnet motors and switched reluctance motors capabilities for electric and hybrid electric vehicles," in *Proc. IEEMA Engineer Infinite Conf.*, 2018, pp. 1–5, doi: 10.1109/ETECHNXT.2018.8385282.

[11] D. S. M. Osheba, A. Nazih, and A. S. Mansour, "Performance enhancement of PV system using VSG with ANFIS controller," *Elect. Eng.*, vol. 105, no. 5, pp. 1–15, 2023, doi: 10.1007/s00202-023-01824-4.

[12] M. Hamouda and L. Számel, "Reduced torque ripple based on a simplified structure average torque control of switched reluctance motor for electric vehicles," in *Proc. Int. IEEE Conf. Workshop Obuda Elect. Power Eng. (CANDO-EPE)*, Nov. 2018, pp. 109–114, doi: 10.1109/CANDO-EPE.2018.8601133.

[13] X. Tian, Y. Cai, X. Sun, Z. Zhu, Y. Wang, and Y. Xu, "Incorporating driving style recognition into MPC for energy management of plug-in hybrid electric buses," *IEEE Trans. Transport. Electrific.*, vol. 9, no. 1, pp. 169–181, Mar. 2023, doi: 10.1109/TTE.2022.3181201.

[14] M. Hamouda, F. Al-Amyal, I. Odinaev, M. N. Ibrahim, and L. Számel, "A novel universal torque control of switched reluctance motors for electric vehicles," *Mathematics*, vol. 10, no. 20, p. 3833, Oct. 2022, doi: 10.3390/math10203833.

[15] L. Kalaivani, P. Subburaj, and M. Willjuice Iruthayarajan, "Speed control of switched reluctance motor with torque ripple reduction using non-dominated sorting genetic algorithm (NSGA-II)," *Int. J. Electr. Power Energy Syst.*, vol. 53, pp. 69–77, Dec. 2013, doi: 10.1016/j.ijepes.2013.04.005.

[16] J. Mukhopadhyay, S. Choudhuri, and S. Sengupta, "ANFIS based speed and current control with torque ripple minimization using hybrid SSD-SFO for switched reluctance motor," *Sustain. Energy Technol. Assessments*, vol. 49, Feb. 2022, Art. no. 101712, doi: 10.1016/j.seta.2021.101712.

[17] P. Ramesh and P. Subbaih, "Design and control of SR drive system using ANFIS," in *Proc. Int. Conf. Elect., Electron., Optim. Techn. (ICEEOT)*, 2016, pp. 3815–3819, doi: 10.1109/ICEEOT.2016.7755428.

[18] K. Lakshmanan, S. Perumal, and W. I. Mariasiluvairaj, "Artificial intelligence-based control for torque ripple minimization in switched reluctance motor drives," *Acta Scientiarum. Technol.*, vol. 36, no. 1, pp. 33–40, Dec. 2013, doi: 10.4025/actascitechnol.v36i1.18097.

[19] H. Kotb, A. H. Yakout, M. A. Attia, R. A. Turky, and K. M. Abo-Ras, "Speed control and torque ripple minimization of SRM using local unimodal sampling and spotted hyena algorithms based cascaded PID controller," *Ain Shams Eng. J.*, vol. 13, no. 4, Jun. 2022, Art. no. 101719, doi: 10.1016/j.asej.2022.101719.

[20] R. Sehab, A. Akrad, and Y. Saadi, "Super-twisting sliding mode control to improve performances and robustness of a switched reluctance machine for an electric vehicle drivetrain application," *Energies*, vol. 16, no. 7, p. 3212, Apr. 2023, doi: 10.3390/en16073212.

[21] M. R. D. C. Reis, W. R. H. de Araujo, V. M. Gomes, F. D. S. e Silva, C. A. Ganzaroli, F. A. Gomes, G. A. Wainer, and W. P. Calixto, "Optimized techniques for driving and control of the switched reluctance motor to improve efficiency," *Control Eng. Pract.*, vol. 90, pp. 1–18, Sep. 2019, doi: 10.1016/j.conengprac.2019.06.007.

[22] R. Krishnan, *Switched Reluctance Motor Drives: Modeling, Simulation, Analysis, Design, and Applications*. Boca Raton, FL, USA: CRC Press, 2017, doi: 10.1201/9781420041644.

[23] F. Al-Amyal, M. Hamouda, and L. Számel, "Performance improvement based on adaptive commutation strategy for switched reluctance motors using direct torque control," *Alexandria Eng. J.*, vol. 61, no. 11, pp. 9219–9233, Nov. 2022, doi: 10.1016/j.aej.2022.02.039.

[24] H. Oubouaddi, A. Brouri, and A. Ouannou, "Speed control of switched reluctance machine using fuzzy controller and neural network," in *Proc. Int. Conf. Intell. Syst. Comput. Vis. (ISCV)*, 2022, pp. 1–6, doi: 10.1109/ISCV54655.2022.9806121.

[25] A. Abdelmaksoud, M. A. Gaafar, M. Orabi, H. Chen, and M. Dardeer, "Performance investigation of switched reluctance motor drive system under firing angles variation," in*Proc. IEEE Conf. Power Electron. Renew. Energy (CPERE)*, Feb. 2023, pp. 1–8, doi: 10.1109/CPERE56564.2023.10119624.

PEMMAREDDY SAITEJA received the M.Tech. degree in mechanical engineering from Jawaharlal Nehru Technological University Anantapur, Anantapur. He is currently pursuing the Ph.D. degree with the Vellore Institute of Technology (VIT), Vellore, Tamil Nadu. His Ph.D. research focuses mainly on control system development for electric motors used in electric vehicles. His research interests include energy management systems, noise and vibration analysis, and control in electric motors.

BRAGADESHWARAN ASHOK received the Ph.D. degree from the School of Mechanical Engineering, Vellore Institute of Technology (VIT), Vellore, in 2017. He is currently an Associate Professor with the Department of Automotive Technology, School of Mechanical Engineering, VIT. His research interests include automotive engineering, electric and hybrid vehicle powertrain calibration, IC engines, and automotive electronics. His research work is aimed at motor control algorithm development for electric vehicle applications. He has been awarded as a ''Top 2% Scientist in the world'' by a study conducted by researchers at Stanford University recently.

BYRON MASON received the B.Eng. degree in mechanical engineering and the Ph.D. degree in powertrain calibration and control from the University of Bradford, Bradford, U.K., in 2005 and 2009, respectively. He is currently a Senior Lecturer in intelligent powertrain systems with the Department of Aeronautical and Automotive Engineering, Loughborough University, Loughborough, U.K.

S. KRISHNA received the B.E. degree in electronics and communication and the M.Tech. and Ph.D. degrees in mechatronics from the Vellore Institute of Technology (VIT), Vellore. He is currently an Assistant Professor with the Automotive Division, VIT. His research interests include automotive steering systems, electric vehicles, and modern control systems.